Journal of Physiology (1992), **448**, *pp.* 161–188
With 15 figures
Printed in Great Britain

DIHYDROPYRIDINE-SENSITIVE AND ω-CONOTOXIN-SENSITIVE CALCIUM CHANNELS IN A MAMMALIAN NEUROBLASTOMA–GLIOMA CELL LINE

BY HARUO KASAI* AND ERWIN NEHER

From the Abteilung Membranbiophysik, Max Planck Institut für biophysikalische Chemie, am Fassberg, Göttingen, Germany

(*Received 2 May 1991*)

SUMMARY

1. Pharmacological and kinetic properties of high-voltage-activated (HVA) Ca^{2+} channel currents were studied using the whole-cell and perforated patch-clamp methods in a mouse neuroblastoma and rat glioma hybrid cell line, NG108–15, differentiated by dibutyryl cyclic AMP or by prostaglandin E_1 and theophylline.

2. The HVA currents were separated into two components by use of two organic Ca^{2+} channel antagonists, ω-conotoxin GVIA (ωCgTX) and a dihydropyridine (DHP) compound, nifedipine. One current component, I_{DHP}, was blocked by nifedipine (K_d = 8·2 nM) and was resistant to ωCgTX. Conversely, the other component, $I_{\omega CgTX}$, was irreversibly blocked by ωCgTX and was resistant to DHPs. Thus, I_{DHP} could be studied in isolation by a short application of ωCgTX, while $I_{\omega CgTX}$ could be studied in the presence of nifedipine.

3. The voltage for half-activation of I_{DHP} was smaller than that of $I_{\omega CgTX}$ by 13 mV. I_{DHP} was activated at potentials that were subthreshold for voltage-dependent K^+ currents of the cell, whereas $I_{\omega CgTX}$ was not.

4. Time courses of activation and deactivation of I_{DHP} were faster than those of $I_{\omega CgTX}$.

5. Voltage-dependent inactivation was small for both I_{DHP} and $I_{\omega CgTX}$ at any potential.

6. Ca^{2+}-dependent inactivation of I_{DHP} was faster and more prominent than that of $I_{\omega CgTX}$. The time course of the Ca^{2+}-dependent inactivation of I_{DHP}, but not $I_{\omega CgTX}$, was slowed as the membrane potential was made more positive between −20 and 30 mV, although amplitude of the current was increased.

7. Alkaline earth metal ions carried the two components of I_{HVA} in the same order: $Ba^{2+} > Sr^{2+} > Ca^{2+}$.

8. Metal ions blocked the two components of I_{HVA} in the same order of potency: $Gd^{3+} > La^{3+} > Cd^{2+} > Cu^{2+} > Mn^{2+} > Ni^{2+}$.

9. An alkylating agent, *N*-ethylmaleimide (NEM, 0·1 mM), selectively augmented I_{DHP} by 30%.

* Present address: Department of Physiology, Faculty of Medicine, University of Tokyo, Hongo, Bunkyo-ku, Tokyo, 113 Japan.

MS 9365

10. During the course of cellular differentiation induced by dibutyryl cyclic AMP, I_{DHP} appeared earlier than $I_{\omega CgTX}$.

11. These results indicate that two classes of Ca^{2+} channels contribute to the HVA currents of this cell line. The DHP-sensitive channel is more apt to generate Ca^{2+} spikes and Ca^{2+} plateau potentials than the ωCgTX-sensitive channel.

INTRODUCTION

Voltage-dependent Ca^{2+} channels in plasma membranes play key roles in triggering elevation of cytosolic Ca^{2+} level in excitable cells. Co-existence of two classes of Ca^{2+} channels have been reported in wide varieties of cells (Carbone & Swandulla, 1989; Bean, 1989; Hess, 1990). One class is activated by small depolarizations and subsequently inactivated (low-voltage-activated, LVA, T-current), while the other is activated by larger depolarizations and shows less inactivation (high-voltage-activated, HVA). Pharmacological properties of these two classes of Ca^{2+} channels are also distinctive. The HVA current is potently blocked by Cd^{2+}, while the LVA current is blocked by Ni^{2+}. Further, the HVA currents of muscles are specifically blocked by dihydropyridine compounds (DHPs).

Further heterogeneity in Ca^{2+} channels has been suggested in vertebrate neurones, because only a small part of the HVA current is blocked DHPs (Miller, 1984). In chick DRG neurones, a type of HVA Ca^{2+}-channel current ('N-type') which is resistant to DHPs and which has single-channel properties different from the DHP-sensitive one ('L-type') has been found (Nowycky, Fox & Tsien, 1985; Fox, Nowycky & Tsien, 1987*b*). The 'N-type' current was also characterized as the inactivating component of the HVA current, while the 'L-type' current as the long-lasting component (Fox, Nowycky & Tsien, 1987*a*; Tsien, Lipscombe, Madison, Bley & Fox, 1988). The latter conclusion, however, did not account for pharmacological observations of HVA currents made by other groups on the same neurones (Boll & Lux, 1985; Kasai, Aosaki & Fukuda, 1987; Swandulla & Armstrong, 1988). These and other findings raised the question of whether or not there were multiple components in the HVA current (Carbone & Lux, 1987; Swandulla & Armstrong, 1988).

Subsequent work has shown that a toxin of a marine snail, ω-conotoxin GVIA (ωCgTx) (Gray, Olivera & Cruz, 1988), irreversibly blocks the component of HVA current which is resistant to DHPs, while the actions of this toxin on DHP-sensitive current and LVA current is weak (Kasai, 1987; Kasai *et al.* 1987; Aosaki & Kasai, 1989; Plummer, Logothetis & Hess, 1989; Carbone, Sher & Clementi, 1990; Regan, Sah & Bean, 1991). These pharmacological findings provide a more robust means of identifying one population of Ca^{2+} channels which is resistant to DHPs and offer a convenient way to isolate this population in physiological experiments. In addition, these studies have clarified another important issue for identification of the current components: inactivation kinetics is not a suitable tool to separate the two HVA currents. (Aosaki & Kasai, 1989; Carbone *et al.* 1990).

However, detailed comparison between the properties of the two HVA Ca^{2+} channels has been hampered by the relative sparsity of DHP-sensitive current in primary neurones (Aosaki & Kasai, 1989). For this reason, we have studied a mouse neuroblastoma and rat glioma hybrid cell line, NG108–15. We have found that the

HVA current of this cell comprises two components, one ωCgTX-sensitive and the other DHP-sensitive, as is the case with the Ca^{2+} channels in other cells. Based on this separation, we have studied the activation, inactivation, and permeability properties of these channels as well as their block by metal ions. Systematic differences in some of these properties suggest distinctive functional roles for these channels in neurones. Preliminary results of these experiments have been reported in abstract form (Kasai, 1989).

METHODS

Cell culture

NG108–15 cells (line 108cc15 from Dr B. Hamprecht, Tuebingen, Germany) were stored under liquid nitrogen, and retrieved into culture flasks every 2 months. The culture medium was composed of 90% DMEM (Dulbecco's modified Eagle's medium), 10% FCS (fetal calf serum), HAT (hypoxanthine–aminopterin–thymidine) supplement (Sigma, St Louis, USA) and penicillin–streptomycin. Two days prior to differentiation, the cells were transferred to cultured plates containing glass cover-slips. Electrophysiological experiments were made with these plates. To induce cell differentiation, the cells in the culture plates were supplied with a low-serum growth medium composed of 98% DMEM, 1% FCS, HAT and the antibiotics. One of the following factors was added: factor A: 1 mM-dibutyryl cyclic AMP (with 5 mg l^{-1} insulin, 100 mg l^{-1} transferrin, 16 mg l^{-1} putrescine, 5·2 μg l^{-1} Na_2SeO_3, 6·3 μg l^{-1} progesterone); factor B: 10 μM-prostaglandin E_1 and 1 mM-theophylline. The cells were used for experiments 3–6 days after the differentiation treatment, unless otherwise stated. For the whole-cell experiments, it was essential to use the cells without neurites. These cells were more frequently found in the cells treated with factor B (Hamprecht, 1977). The basic properties of Ca^{2+} channel currents described in this paper were not different in the cells treated with factors A and B (but see Kasai, 1992).

Solutions

The composition of solutions used in this study is listed in Table 1. The whole-cell patch-clamp (Hamill, Marty, Neher, Sakmann & Sigworth, 1981) was performed in Ba^{2+} external solution, unless otherwise stated. For recording Ca^{2+} or Sr^{2+} current through Ca^{2+} channels, we used external solutions in which sodium and potassium were substituted with tetraethylammonium (TEA) to suppress K^+ currents effectively. Patch pipettes were filled with the Cs^+ solution. Ca^{2+} concentration in the internal solutions was chelated to 10^{-8} M by using EGTA. For recording K^+ currents as well as Ca^{2+} currents, the cells were bathed in Ca^{2+} Ringer solution and patch pipettes were filled with K^+ solution. All experiments were performed at room temperature (22–25°C).

The perforated patch method (Horn & Marty, 1988) was applied to make stable long-term recordings of the Ca^{2+} channel currents. Nystatin (Sigma) was first dissolved into dimethylsulphoxide (DMSO) at 50 mg ml^{-1} and then diluted into the Cs^+ solution. Patch pipettes were filled in a two-stage process: the tip of the pipette was filled with the Cs^+ solution without nystatin, and the remainder of the pipette was then back-filled with the Cs^+ solution containing 200–300 μg ml^{-1} nystatin.

Drugs

The dihydropyridine compounds, nifedipine and Bay K 8644 (Bayer, Leverkusen, Germany), were dissolved in DMSO at 5 mM. Synthetic ω-conotoxin GIVA (Peptide Institute, Minoh, Osaka, Japan) was dissolved in distilled water 200 μM. *N*-Ethylmaleimide (NEM, Sigma) was dissolved into water at 100 mM. NEM was used within 6 h after making the stock solution. These drugs and metal ions (Gd^{3+}, La^{3+}, Cd^{2+}, Cu^{2+}, Mn^{2+}, and Ni^{2+}) were diluted into the Ba^{2+} solution and applied onto the cell using puffing pipettes (tip diameter ~ 4 μM) with positive pressure (10–20 cmH_2O).

Recordings

Ca^{2+} channels currents were measured using either an EPC-7 patch-clamp amplifier (List Electronics, Darmstadt, Germany) or EPC-9 patch-clamp amplifier (HEKA Electronics, Lambrecht/Pfalz, Germany). They were low-pass filtered (3 kHz), sampled at 5 kHz, and analysed by a digital computer. To eliminate capacitative transient and leakage currents, a P/4 procedure was used (Armstrong & Bezanilla, 1977), which was performed at −80 mV. Unless otherwise described, membrane potential was held at −40 mV where the LVA current was almost completely

inactivated (Fig. 1). In most experiments, 10 mM-Ba^{2+} was used as the charge carrier instead of Ca^{2+}, since the HVA current was larger in Ba^{2+} and devoid of Ca^{2+}-dependent inactivation (Fig. 9). Pipette resistance ranged between 2 and 5 MΩ, and series resistance between 4 and 6 MΩ. For the analysis of activation kinetics (Figs 3–6), the speed of the voltage clamp was improved by (1) choosing cells with membrane capacitance smaller than 60 pF, (2) using larger patch pipette

TABLE 1. Compositions of solutions. The first column gives symbols which are used in the text to indicate the respective solution

External solution	Divalent cation (mM)	NaCl (mM)	TEACl (mM)	KCl (mM)	$MgCl_2$ (mM)	Glucose (mM)	TTX (μM)	Na-HEPES (mM)	pH
Ba^{2+}	10 $BaCl_2$	145	0	5·5	1	10	0·1	10	7·2
Ca^{2+}	10 $CaCl_2$	0	150	0	1	10	0·1	10	7·2
Sr^{2+}	10 $SrCl_2$	0	150	0	1	10	0·1	10	7·2
Ca^{2+} Ringer	10 $CaCl_2$	145	0	5·5	1	10	0·1	10	7·2

Internal solution	CsCl (mM)	KCl (mM)	$MgCl_2$ (mM)	Na-EGTA (mM)	Ca-EGTA (mM)	ATP (mM)	Na-HEPES (mM)	pH
Cs^+	145	0	1	11	1	1	10	7·2
K^+	0	145	1	11	1	1	10	7·2

(around 1 MΩ) to reduce the series resistance (less than 2 MΩ), and (3) electronically compensating for the series resistance by 70%. An estimated speed of clamp in these recording configuration was faster than 36 μs (= 0·3 × 60 pF × 2 MΩ), which is sufficiently fast for studying a tail current with a time constant around 360 μs (Fig. 4*C*). These data were low-pass filtered (10 kHz) and sampled at 20 kHz. A digital computer was used to fit theoretical equation to current traces with the least-squares fit method.

RESULTS

Two components of HVA currents

Ca^{2+} channel currents of NG108–15 cells were made of two major components, low-voltage-activated current (I_{LVA}) and high-voltage-activated current (I_{HVA}), as described previously (Tsunoo, Yoshii & Narahashi, 1986). In the experiment shown in Fig. 1*A*, examining currents in Ba^{2+} solution, the two current components were activated by double pulses. At the first pulse, the membrane potential was depolarized to −20 mV for 200 ms to activated I_{LVA}, and then, after 50 ms hyperpolarization to −40 mV, it was depolarized to 0 mV. I_{LVA} was inactivated during the first depolarizing pulse (Fig. 1*A*), the current activated by the second command was mostly I_{HVA}. In contrast to I_{LVA}, I_{HVA} did not show marked decay during depolarization. In Fig. 1*B*, the peak amplitudes of I_{LVA} and I_{HVA} are plotted against holding membrane potentials (V_h). The I_{LVA} was markedly reduced at depolarized V_h, which is consistent with I_{LVA} in other cells (Carbone & Swandulla, 1989), except that the complete inactivation of I_{LVA} in the neuroblastoma cell was attained at 10–20 mV more positive potential (−40 mV) than in other cells (Tsunoo *et al.* 1986; Narahashi, Tsunoo & Yoshii, 1987). By contrast, I_{HVA} barely depended on V_h. The apparent lack of the V_h-dependent inactivation in I_{HVA} was not due to the pre-pulse (−20 mV), since the same observation was made if I_{HVA} was activated with a single pulse to 0 mV in cells devoid of I_{LVA} (data not shown). Thus, I_{HVA} of this cell could be classified as 'L-type' (Tsien *et al.* 1988), because it was long-lasting and did not depend on V_h.

The heterogeneity in the I_{HVA} was first revealed using two organic Ca^{2+} channel antagonists, dihydropyridine (DHP) compounds and ω-conotoxin GVIA (ω-CgTX). First, a DHP antagonist, nifedipine, blocked only a part of I_{HVA} (Fig. 2*A* and *B*) which was evoked by a depolarization pulse to 0 mV from a V_h of −40 mV. The

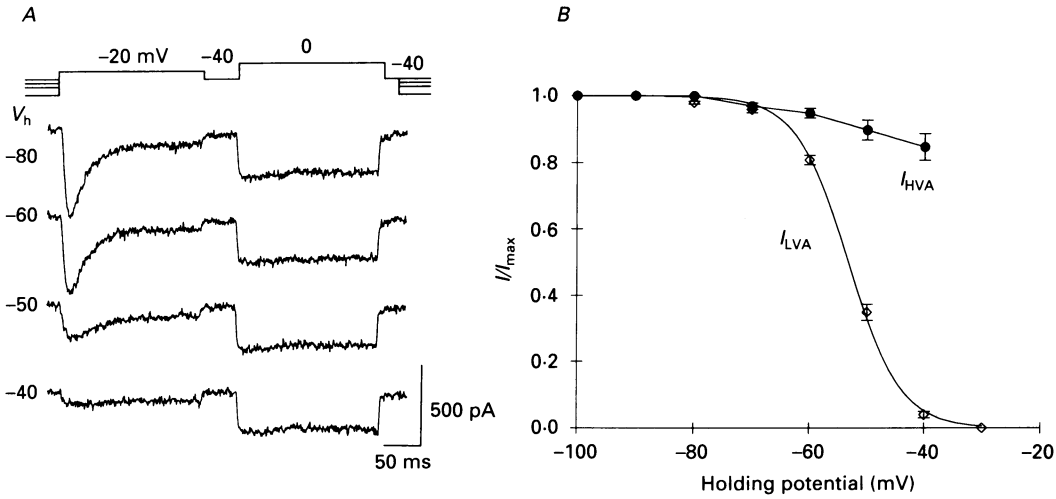

Fig. 1. Low-voltage-activated currents (I_{LVA}) and high-voltage-activated currents (I_{HVA}) recorded from differentiated NG108–15 cells in Ba^{2+} solution (10 mM-Ba^{2+}, Table 1). *A*, current traces evoked by sequential depolarizing pulses to −20 mV and to 0 mV. The holding potential (V_h) was varied between −80 and −40 mV. The voltage commands are shown in the uppermost traces. *B*, V_h dependence of I_{LVA} and I_{HVA}. I_{HVA} was measured as an inactivating component of the current evoked at −20 mV and I_{HVA} as the current at the second pulse to 0 mV. Amplitudes of the currents were normalized with respect to the currents evoked from V_h of −80 or −100 mV. Each point represents the mean ± S.E.M. from five cells.

fraction blocked was variable from cell to cell (0–100 %, mean 62 %, S.D. = 15 %, $n = 20$). The block was more than 95 % complete in 30 % of the cells. Second, ωCgTX irreversibly blocked only a part of I_{HVA} (Fig. 2*A* and *B*): its effect was also variable (0–90 %, mean 30 %; S.D. = 11 %, $n = 60$). Third, nifedipine blocked most of the I_{HVA} that was left after the application of ωCgTX (Fig. 2*A* and *B*) (80–98 % block, mean = 92 %, S.D. = 4 %, $n = 57$). These data suggest that there are two I_{HVA} components with different sensitivities to DHP and ωCgTX.

We examined whether there was a DHP-sensitive current which was irreversibly blocked by ωCgTX. Figure 2 depicts results representative of seven experiments where the effect of nifedipine was tested before and after application of ωCgTX. The perforated patch method (Methods) was used to record I_{HVA} stably for a long recording period. Peak amplitudes of I_{HVA} were monitored every 30 s at 0 mV. The first application of nifedipine reversibly reduced the current by 59 %, whereas ωCgTX irreversibly blocked the current by 32 % (Fig. 2*B*). The second application of nifedipine reduced the current by an amount (56 % of initial amplitude) almost equal to the first application, suggesting that ωCgTX does not block the nifedipine-sensitive current (Fig. 2*B*). We further confirmed this by comparing the effects of

nifedipine on current–voltage (I–V) relationships before (Fig. 2C) and after (Fig. 2D) ωCgTX application. Figure 2E plots reductions of the currents by nifedipine, indicating that DHP-sensitive currents were not significantly affected by ωCgTX at any potential. Note that nifedipine blocked the I_{HVA} evoked by small depolarizations

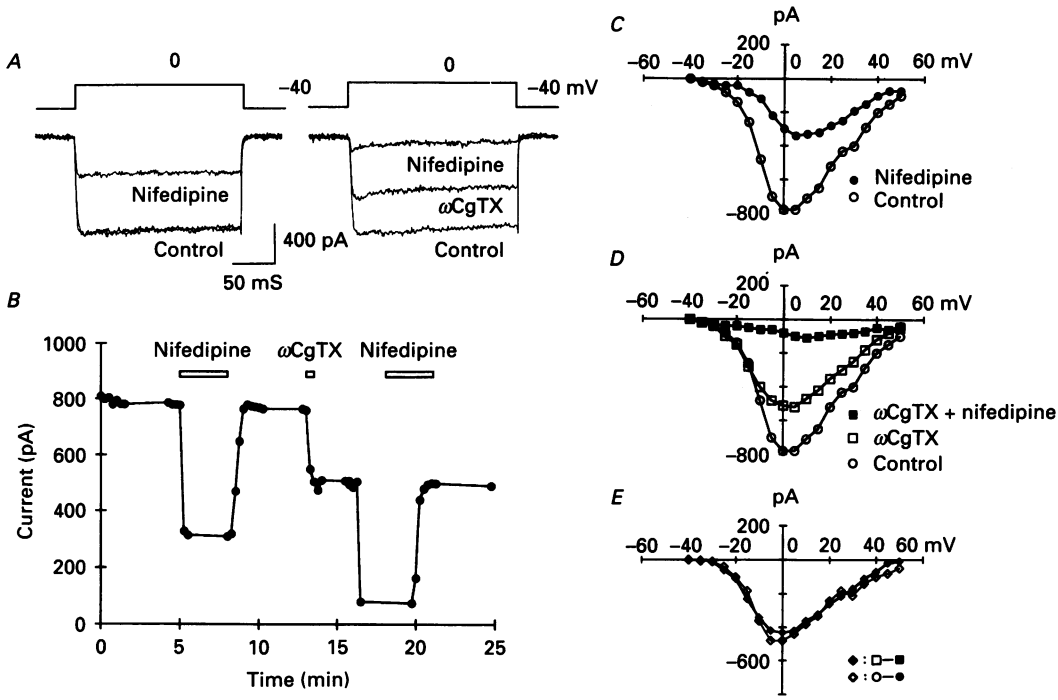

Fig. 2. Pharmacological separation of the two I_{HVA}s. I_{HVA} was recorded from a cell using the perforated patch method in Ba^{2+} solution. The holding potential was −40 mV. Actions of nifedipine (5 μM) on the I_{HVA} were compared before and after application of ω-conotoxin GVIA (ωCgTX, 10 μM). A, blocking effects of the Ca^{2+} antagonists on the I_{HVA} evoked at 0 mV. Current traces before, during and after application of nifedipine were superimposed in the left traces, and those before, after ωCgTX application and during the second application of nifedipine in the right traces. B, changes in peak amplitude of the I_{HVA} during the sequential application of nifedipine and ωCgTX. Application periods of the drugs were indicated by open bars. C and D, current–voltage (I–V) relationships obtained before the drug application (○ in C and D), during the first application of nifedipine (●, C), after application of ωCgTX (□, D) and during the second application of nifedipine (■, D). E, decrements in I_{HVA} caused by nifedipine before (◇) and after (◆) the ωCgTX application.

($\leqslant -20$ mV) (Fig. 2C and D), while ωCgTX did not (Fig. 2D). This indicates that the nifedipine-sensitive current can be activated with a smaller depolarization than the ωCgTX-sensitive one (see below).

Separation of I_{DHP} and $I_{\omega CgTX}$

We define the ωCgTX-sensitive component of current ($I_{\omega CgTX}$) as the I_{HVA} which is irreversibly blocked by ωCgTX and the DHP-sensitive component of current (I_{DHP}) as the one which is blocked by nifedipine. I_{DHP} was separated by treating the

cells with ωCgTX (10 μM for 30 s), while $I_{\omega CgTX}$ was examined in the presence of nifedipine. There were two sources of errors in this procedure. First, nifedipine did not completely block I_{HVA} left after ωCgTX treatment (Figs 2*B* and 11*D*), and hence current recorded in the presence of nifedipine is not a pure $I_{\omega CgTX}$. The DHP- and

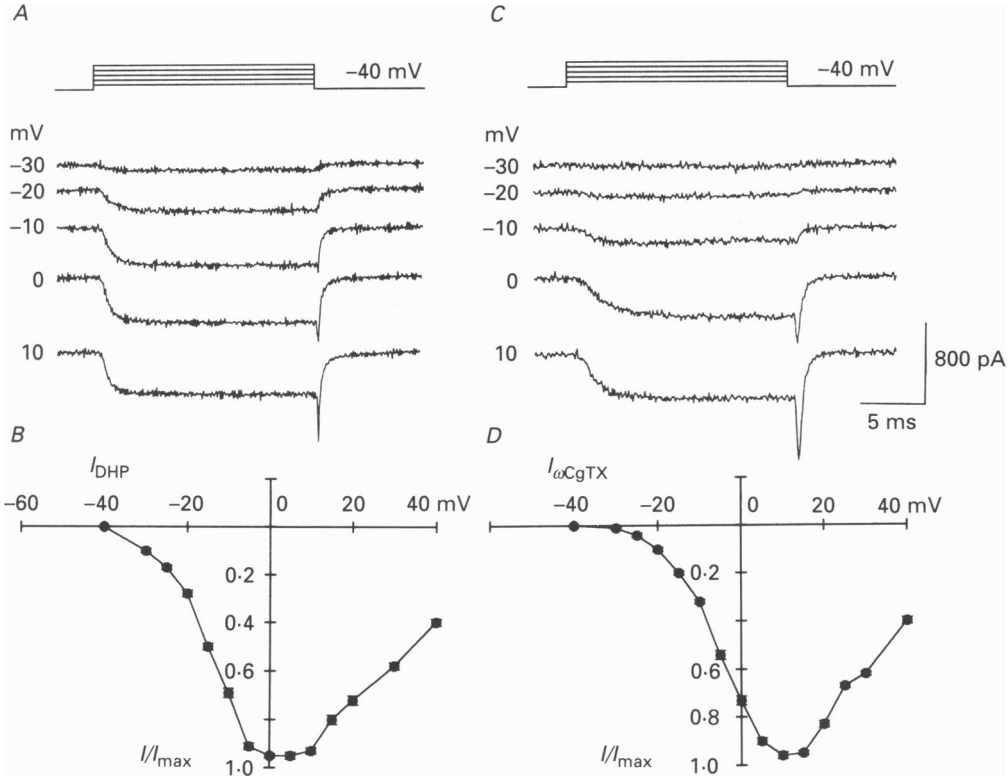

Fig. 3. *I–V* relationships of I_{DHP} and $I_{\omega CgTX}$. Each of the two I_{HVA}s were pharmacologically separated in Ba^{2+} solution in two different cells. *A* and *C*, I_{DHP} (*A*) and $I_{\omega CgTX}$ (*C*) evoked by step depolarizations to several potential indicated at the left side of the traces. *B* and *D*, *I–V* relationships of I_{DHP} (*B*) and $I_{\omega CgTX}$ (*D*) obtained from peak amplitudes during depolarization pulses. Each point represents a mean ± S.E.M. of five or six experiments. Most of the error bars are occluded by the symbol.

ωCgTX-resistant current, however, was always small and proportional to I_{DHP} (2–20%, mean = 8%). For studying $I_{\omega CgTX}$, we therefore used cells which had I_{DHP} less than 40%, since this should make the contamination by the resistant current less than 12% (mean = 5%). Second, the antagonists (nifedipine and ωCgTX) used for separating the current might affect the properties of the I_{HVA}s. We therefore routinely examined the properties of I_{HVA} before application of any drug. In 30% of cells, the I_{HVA} was almost exclusively I_{DHP} and the characteristics of I_{DHP} revealed in this way were consistent with those of I_{DHP} isolated with ωCgTX. When I_{HVA} was composed of both I_{DHP} and $I_{\omega CgTX}$, it invariably displayed properties intermediate between those of I_{DHP} and $I_{\omega CgTX}$. Hence, the differences between the properties of the two I_{HVA}s studied below could not be ascribed to effects of the Ca^{2+} antagonists.

I–V relationships of $I_{\omega CgTX}$ and I_{DHP}

We found that I_{DHP} was more readily activated by depolarization than $I_{\omega CgTX}$. Each of the two I_{HVA}s was separated pharmacologically in different cells and evoked by command pulses to several potentials (Fig. 3*A*). The following differences were

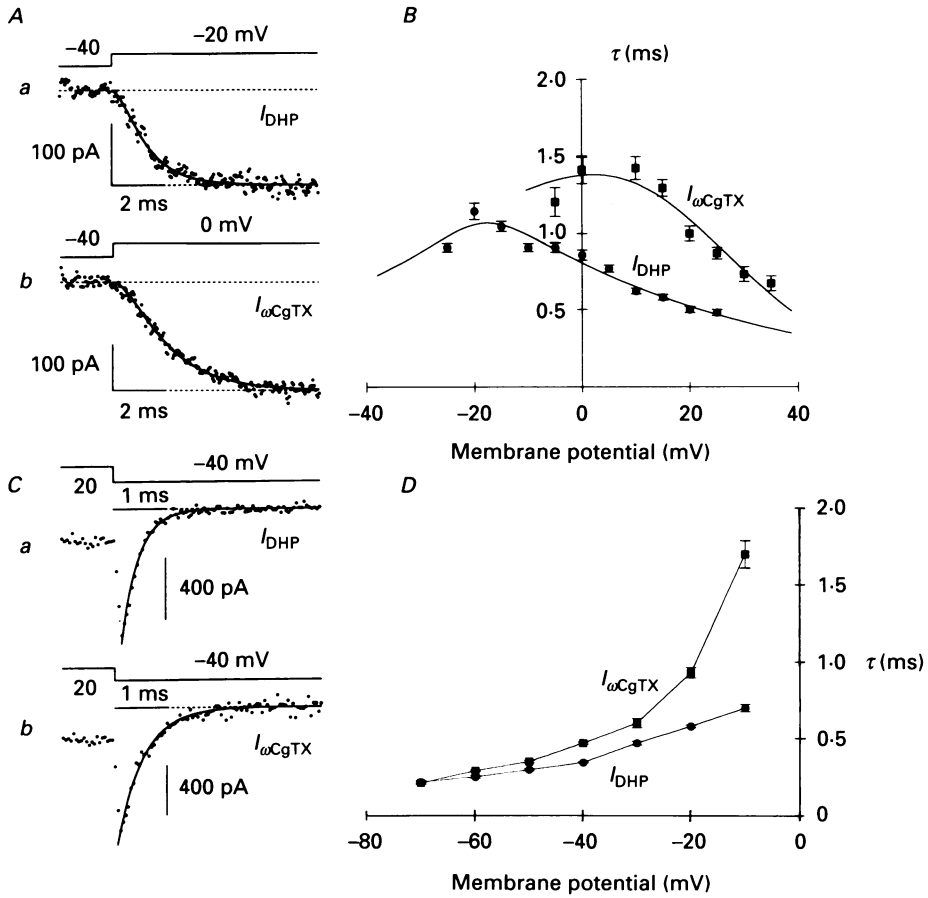

Fig. 4. Time courses of the activation and deactivation of I_{DHP} and $I_{\omega CgTX}$. *A*, onsets of I_{DHP} (*a*) and $I_{\omega CgTX}$ (*b*) upon depolarization fitted with the Hodgkin–Huxley model. Both of I_{HVA}s were fitted with $I\{1-\exp(-t/\tau)\}^2$, where I was 130 and 205 pA, and τ was 1·0 and 1·7 ms, for *a* and *b*, respectively. *B*, voltage dependence of the time constants (τ) of the activation of I_{DHP} (●) and of $I_{\omega CgTX}$ (■). Each data point represents a mean ± S.E.M. from four to six experiments. Smooth curves were drawn according to an equation: $\tau = 1/(\alpha+\beta)$, where α and β were obtained in Fig. 15. *C*, tail currents of I_{DHP} (*a*) and $I_{\omega CgTX}$ (*b*) at −40 mV fitted with single exponential curves. τ values were 0·28 and 0·41 ms for I_{DHP} and $I_{\omega CgTX}$, respectively. *D*, voltage dependence of τ of the deactivation of I_{DHP} (●) and $I_{\omega CgTX}$ (■). Each data point represents a mean ± S.E.M. of five or six experiments.

noticed. (1) The activation threshold was more negative for I_{DHP} than $I_{\omega CgTX}$; I_{DHP} was already large at −20 mV (Fig. 3*A*, 45% of the maximum), a potential where $I_{\omega CgTX}$ was minimal (Fig. 3*C*, 10% of the maximum). (2) Half-maximal current was attained at a more negative potential for I_{DHP} (−16 mV) than for $I_{\omega CgTX}$ (−6 mV)

(Fig. 3*B* and *D*). (3) The time course of activation was faster for I_{DHP} than for $I_{\omega CgTX}$, which can most clearly be seen in the current trace at 0 mV in Fig. 3*A* and *C*. (4) Tail currents elicited upon repolarization to V_h (−40 mV) were terminated faster in I_{DHP} than in $I_{\omega CgTX}$ (Fig. 3*A* and *C*).

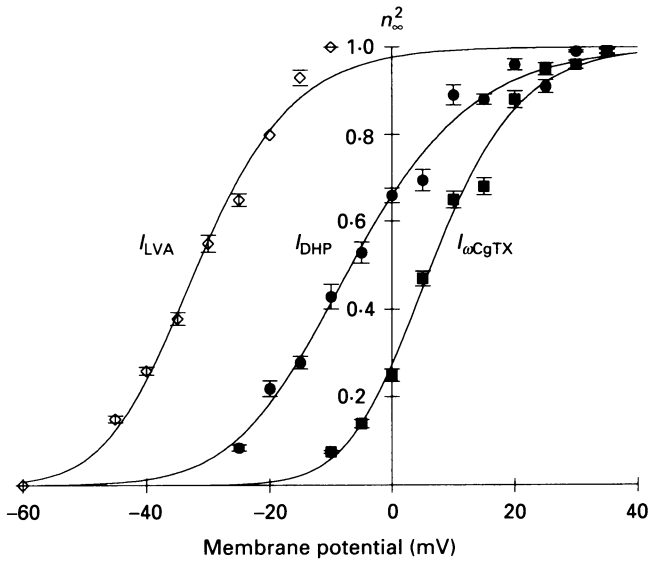

Fig. 5. Activation curves of I_{LVA} (◇), I_{DHP} (●) and $I_{\omega CgTX}$ (■). Tail currents were elicited upon repolarization to −40 mV (−70 mV for I_{LVA}) from different depolarization levels. They were fitted with single exponential curves and extrapolated peak amplitudes were normalized by those evoked at +40 mV (−10 mV for I_{LVA}). Data for I_{LVA} were obtained from cells which had small I_{HVA}. Each data point represents a mean ± S.E.M. of five or six experiments. Smooth lines were drawn according to the equation:

$$n_\infty^2 = 1/[1+\{\exp(V-V_m)/k\}]^2,$$

where V represents membrane potential. The parameters are $V_m = -39{\cdot}6$ mV and $k =$ 8·9 mV for I_{LVA}, $V_m = -16{\cdot}8$ and $k = 11{\cdot}5$ for I_{DHP}, and $V_m = -0{\cdot}77$ and $k = 8{\cdot}22$ for $I_{\omega CgTX}$.

Kinetic differences between these two components allowed their discrimination in recording of I_{HVA}. Treatment with ωCgTX spared the currents evoked at small depolarizations (Fig. 2*D*), and hastened onset and tail currents of I_{HVA}. Thus, the higher activation threshold and slower time courses of activation of $I_{\omega CgTX}$ were not due to the nifedipine used to remove I_{DHP}. These differences were studied more quantitatively in the following two sections.

Analysis of activation and deactivation kinetics

Figure 4*A* shows the two I_{HVA}s evoked at potentials where they were slowest to be activated. The current traces were fitted with a model like that of Hodgkin & Huxley (1952), which is the simplest model for explaining the macroscopic gating behaviour of ion channels. Both components of I_{HVA}s showed a sigmoidal onset upon depolarization and were best described by the model when assuming m^2 kinetics (continuous line in Fig. 4*A*). The same fits could be made for current traces evoked

between −20 and 30 mV. $I_{\omega CgTX}$ activated twice as slowly as I_{DHP} in the voltage range between −10 to 30 mV (Fig. 4*B*).

The tail currents of the each component could be fitted with single exponential curves when measured during hyperpolarization to potentials between −70 to −10 mV (Fig. 4*C*). The time constants of these exponentials decreased at more negative potentials (Fig. 4*D*). The time constant of the deactivation for I_{DHP} was smaller than that of $I_{\omega CgTX}$ at any potential, although the differences were more prominent at more depolarized potentials. For example, they were 0·75±0·1 ms (mean±S.E.M., $n = 4$) and 1·7±0·2 ms ($n = 3$) at −10 mV, and 0·32±0·05 ($n = 5$) and 0·45±0·02 ms ($n = 5$) at −40 mV for I_{DHP} and $I_{\omega CgTX}$, respectively.

Voltage dependence of the activation of I_{DHP} and $I_{\omega CgTX}$

Activation curves for two pharmacologically separated components of I_{HVA} were obtained using the tail currents (Fig. 5). I_{DHP} was activated at more negative potential than $I_{\omega CgTX}$, as expected from the *I–V* relationship. Half-activation was attained at −7 and 6 mV for I_{DHP} and $I_{\omega CgTX}$, respectively. It should be noticed that the slope of the activation curve was less steep for I_{DHP} than for $I_{\omega CgTX}$. This may contribute to reducing the threshold for regenerative potential responses caused by I_{DHP}. For comparison, the activation curve of I_{LVA} was obtained in a similar way. I_{LVA} was activated at potentials 20 mV more hyperpolarized than those required for activation of I_{DHP}.

The 13 mV difference between the activation curves of $I_{\omega CgTX}$ and I_{DHP} can result in differences in their contribution to the excitability of the cell. To see if this was true, we examined the voltage dependence of these Ca^{2+} channels with respect to that of K^+ channels. In Fig. 6, whole-cell clamp experiments were made where both outward K^+ current (I_K) and inward Ca^{2+} current (I_{Ca}) was recorded. Current traces in Fig. 6*A* were recorded after ωCgTX treatment, and thus represent the sum of I_{DHP} and I_K. Those in Fig. 6*C* were recorded in the presence of nifedipine and represent $I_{\omega CgTX}$ and I_K. There are substantial differences in the summed currents of I_{Ca} and I_K: peak and steady-state inward currents are substantially larger for $I_{DHP}+I_K$ than for $I_{\omega CgTX}+I_K$. These differences must primarily originate from differences in the I_{Ca}s, because I_Ks isolated using both of the Ca^{2+} antagonists were not very different in their amplitudes (Fig. 6*A b* and *C b*) and in their voltage dependences (Fig. 6*B* and *D*). I_{Ca}s were estimated by subtracting I_K from $I_{Ca}+I_K$ in Fig. 6*A c* and *C c*. There is a 10 mV difference between activation curves (Fig. 6*B* and *D*) of the two I_{Ca}s, although the maximum amplitudes of the currents were similar (Fig. 6*A c* and *C c*). This difference in activation is striking in comparison to activation of I_K: I_{DHP} is activated at more hyperpolarized potential than I_K, while $I_{\omega CgTX}$ starts to activate at a voltage range similar to that of I_K. This accounts for the large observed difference in $I_{Ca}+I_K$. Note that only I_{DHP} appears to decay during depolarization. This may be due to the Ca^{2+}-dependent inactivation of I_{DHP} studied below.

Voltage-dependent inactivation of I_{DHP} and $I_{\omega CgTX}$

Pronounced voltage-dependent inactivation of the 'N-type' current is an important means of distinguishing this current from the 'L-type' current (Tsien *et al.* 1988). We therefore tested whether the two I_{HVA}s showed similar differences in their

inactivation. This was done by examining the effects of pre-pulses on currents evoked by constant test pulses (Fig. 7). Pre-pulses slightly reduced the test currents, regardless of whether these currents were I_{DHP} or $I_{\omega CgTX}$. The reduction had a monotonous dependence on the amplitude of the pre-pulse, being more pronounced

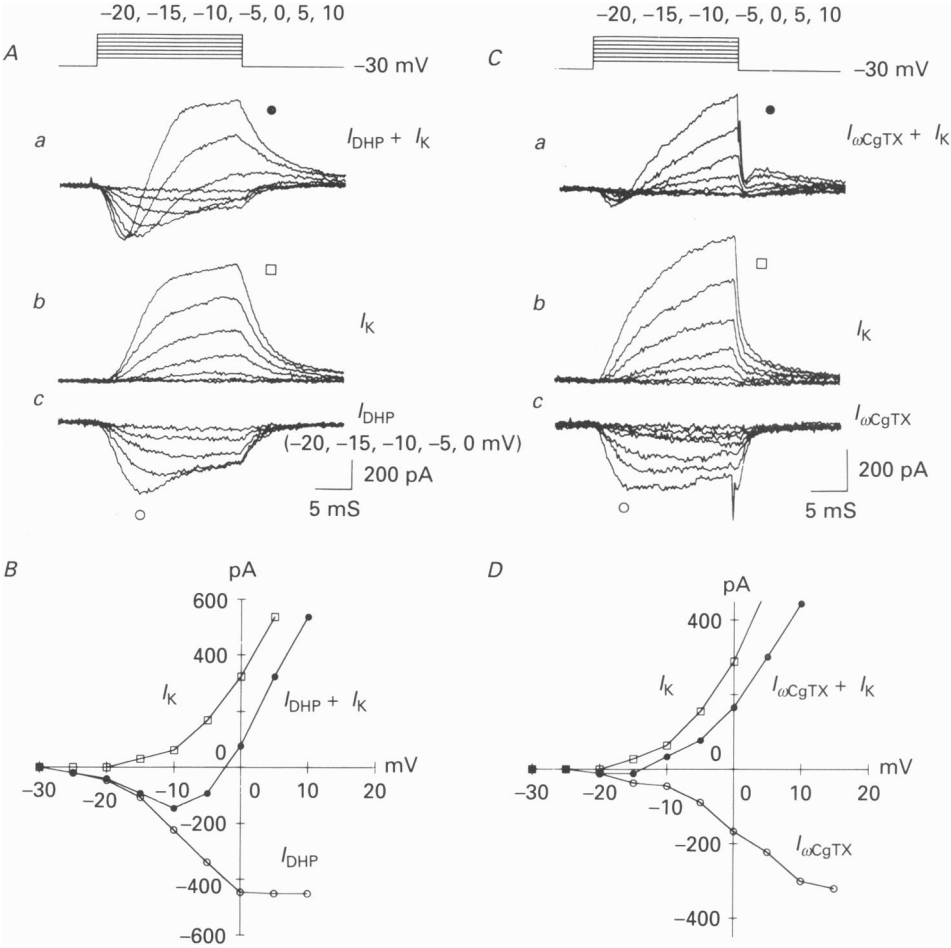

Fig. 6. Mixed HVA Ca^{2+} currents and K^+ currents recorded from two different cells in Ca^{2+} Ringer solution (Table 1). Patch pipettes were filled with K^+ solution (Table 1). V_h was -30 mV. The cells were studied after a short treatment with ωCgTX in *A* and in the presence of nifedipine in *C*. *A* and *C*, superimposed current traces evoked at potentials ranging from -20 to 10 mV. The traces in *a* were composed of I_{Ca} and I_K. In *b*, I_{Ca} was eliminated by nifedipine (*A*) or by ωCgTX (*C*). In *c*, I_{Ca} was estimated by subtracting the traces in *b* from *a*. *B* and *D*, *I–V* relationships of $I_{Ca}+I_K$ (●), I_K (□) and I_{Ca} (○) obtained from data shown in *A* and *C*. Amplitudes of the currents were measured at the end of the depolarization for $I_{Ca}+I_K$ and I_K, and at the peak for I_{Ca}. A half-maximal current was attained at about -10 and 0 mV for I_{DHP} and $I_{\omega CgTX}$, respectively.

at depolarized potentials (Fig. 7*C*). This suggests a voltage-dependent mechanism for inactivation (Chad, 1989). The amount of inactivation was larger for I_{DHP} than for $I_{\omega CgTX}$: 200 ms of depolarization to 0 mV reduced I_{DHP} by 12 ± 3 % (mean $\pm$ S.E.M.,

$n = 6$) and $I_{\omega CgTX}$ by $7 \pm 2\%$ ($n = 5$). The I_{DHP} of this cell was not facilitated by pre-pulses (Fig. 7*A*), unlike DHP-sensitive Ca^{2+} channels of the heart (Lee, 1987) and endocrine cell (Fenwick, Marty & Neher, 1982; Hosi, Rothlein & Smith, 1984).

Ca^{2+}-dependent inactivation of I_{DHP} and $I_{\omega CgTX}$

The decay of I_{DHP} was dramatically increased when Ca^{2+} was used instead of Ba^{2+} as charged carrier (Fig. 8*A*). This inactivation differed in several respects from the

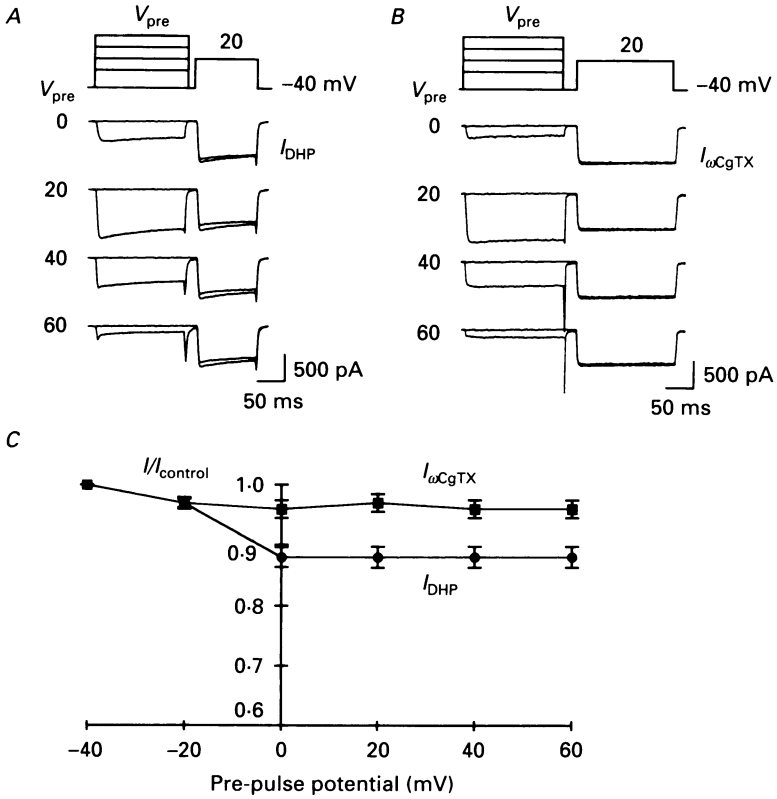

Fig. 7. Voltage-dependent inactivation of I_{DHP} and $I_{\omega CgTX}$. The two I_{HVA}s were separated pharmacologically in Ba^{2+} solution. A double-pulse protocol was used, in which test pulses to a constant potential (20 mV) were preceded by pre-pulses (V_{pre}) with different amplitudes. *A* and *B*, current traces evoked by the double-pulse protocol for I_{DHP} (*A*) and $I_{\omega CgTX}$ (*B*). Current traces with and without pre-pulses were superimposed. The smaller current traces are for cases with pre-pulses. *C*, relative amplitude of test currents, plotted against potentials of pre-pulses, for I_{DHP} (●) and $I_{\omega CgTX}$ (■). Each data point represents a mean ± S.E.M. of four to six experiments.

voltage-dependent inactivation discussed above. First, it was rapid; test current decayed with a time constant of 36 ± 5 ms at 0 mV ($n = 7$). Second, it was more prominent; test currents were greatly (40–50%) reduced by 200 ms long pre-pulses to 0 mV. Finally, the reduction in I_{DHP} was not monotonically dependent on pre-pulse potential. The current was maximally reduced by pre-pulses to 10 to 20 mV

(Fig. 8*C*), a potential range where the current evoked by pre-pulses reached its maximum. Pre-pulses to larger depolarization (Fig. 8*C*) where the pre-pulse–current was smaller caused less reduction. The dependence on permeant ion and the U-shaped dependence on pre-pulse potential indicate that this inactivation is Ca^{2+} dependent (Chad, 1989).

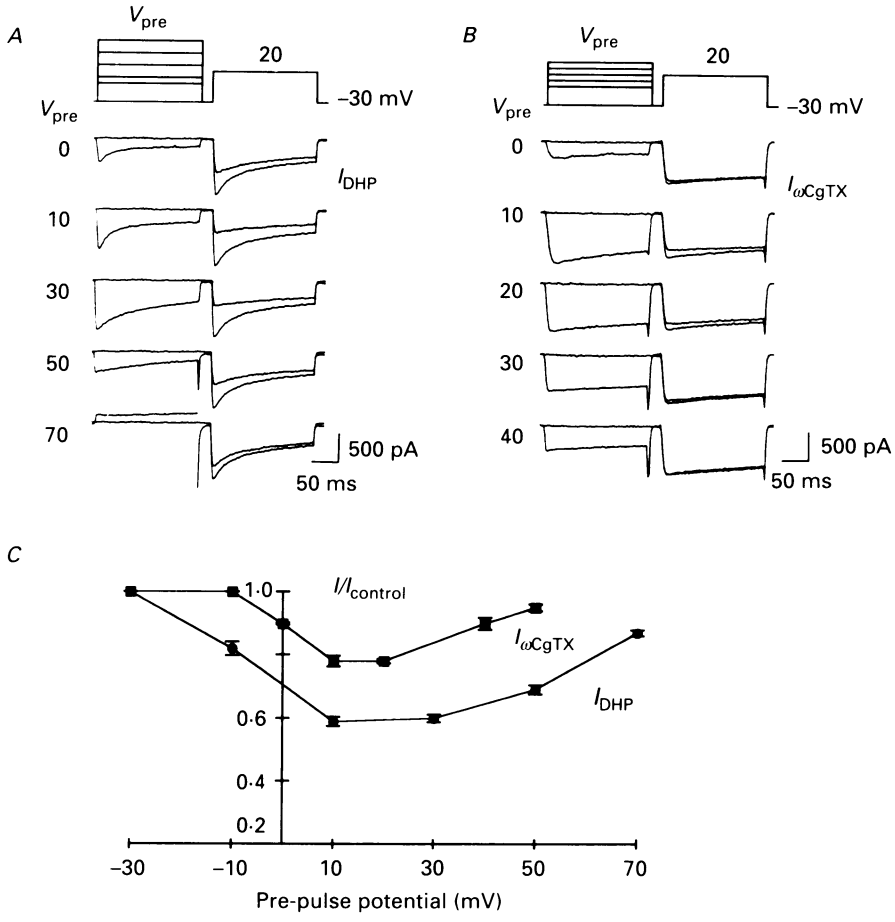

Fig. 8. Ca^{2+} dependence of the inactivation of I_{DHP} and $I_{\omega CgTX}$. The two I_{HVA}s were pharmacologically separated in Ca^{2+} solution (see Table 1). V_h was −30 mV. *A* and *B*, superimposed current traces evoked with the double-pulse protocol for I_{DHP} (*A*) and $I_{\omega CgTX}$ (*B*). *C*, relative amplitudes of the currents plotted against potentials of pre-pulses (V_{pre}) for I_{DHP} (●) and $I_{\omega CgTX}$ (■). Each data point represents a mean ± S.E.M. of five experiments.

The decay of $I_{\omega CgTX}$ also was decreased in Ca^{2+} solution (Fig. 8*B*), although the decay was significantly slower (τ was larger than 100 ms) and smaller (10–20 % than that of I_{DHP}. The inactivation of $I_{\omega CgTX}$ also showed a U-shaped dependence on pre-pulse potential, suggesting that it also was Ca^{2+} dependent. Recovery from Ca^{2+}-dependent inactivation in the case of I_{DHP} was readily reversible, while that of $I_{\omega CgTX}$ was very slow and partly irreversible.

Note that the inactivation time constant of I_{DHP} evoked by a pre-pulse to 0 or 10 mV was smaller than that at 30 mV (Fig. 8*A*), although the amplitude of current at 0 or 10 mV was smaller. This phenomenon was seen in I_{DHP} of every cell examined. In contrast, the inactivation of $I_{\omega CgTX}$ was fastest at 10 mV, where the amplitude of the current is maximal (Fig. 8*B*).

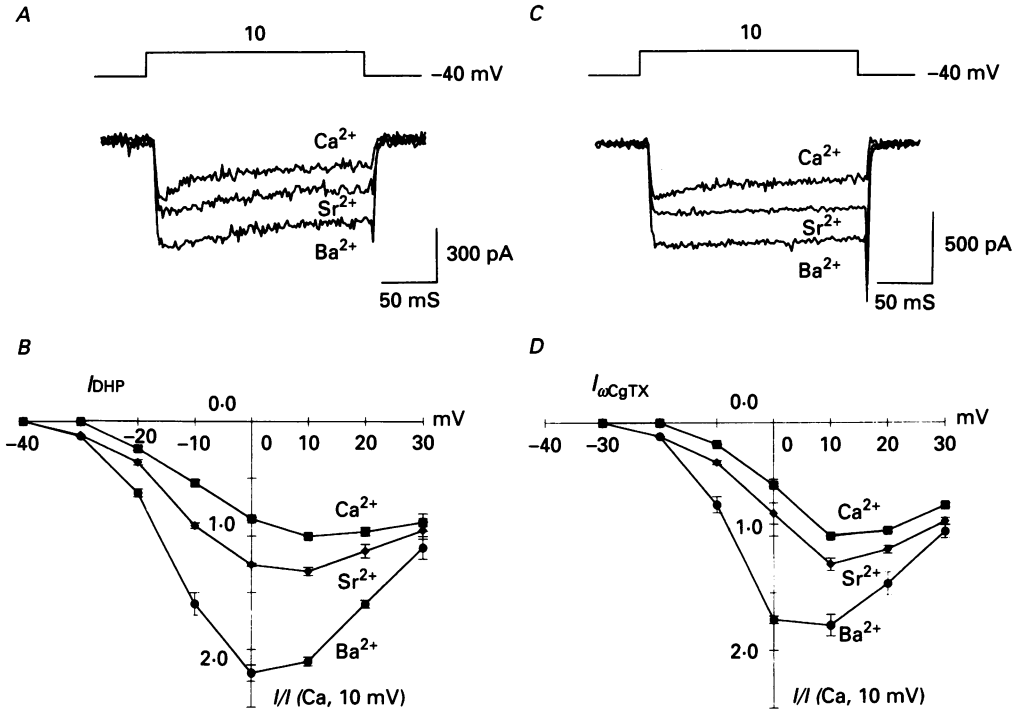

Fig. 9. I_{DHP} and $I_{\omega CgTX}$ carried with Ba^{2+}, Sr^{2+} and Ca^{2+}. The two I_{HVA}s were pharmacologically separated in Ba^{2+} solution and recorded with the perforated patch method. Bathing solutions were quickly superfused and sequentially changed to a Sr^{2+} and then to a Ca^{2+} solution (Table 1). V_h was -30 mV. *A* and *C*, superimposed current traces of I_{DHP} (*A*) or $I_{\omega CgTX}$ (*C*) in three solutions. *B* and *D*, *I–V* relationships in the three solutions for I_{DHP} (*B*) and $I_{\omega CgTX}$ (*D*). I_{HVA} evoked at 10 mV in Ca^{2+} solution was normalized as 1. Each point represents a mean ± S.E.M. from four or five experiments.

I_{DHP} and $I_{\omega CgTX}$ in different permeant ions

When considering I_{LVA}, Ca^{2+} carries larger currents than Ba^{2+}, while, for I_{HVA}, Ba^{2+} carries larger currents than Ca^{2+} (Carbone & Lux, 1987). The two I_{HVA}s, however, did not shown large relative differences in their dependence on the charge carrier. The peak amplitudes of both I_{DHP} and $I_{\omega CgTX}$ were largest in Ba^{2+} solution and smallest in Ca^{2+} solution (Fig. 9*A* and *C*). If the amplitudes of currents evoked at 10 mV are normalized with respect to the amplitudes measured in Ca^{2+} solution, I_{DHP} was 2·1 and 1·3 ($n = 5$) as large in Ba^{2+} and Sr^{2+}, respectively. For the case of $I_{\omega CgTX}$, these values were 1·8 and 1·2 ($n = 4$). The dependence of I_{LVA} and $I_{\omega CgTX}$ on charge carrier might mainly be due to the shift in the activation curve along the voltage axis, because amplitudes of currents were not much affected at strong

depolarizations (30 mV) (Fig. 9*B* and *D*). Further, a clear shift in the *I–V* relationship was detected. Half-maximal I_{DHP} was attained at −17, −15 and −10 mV, for Ba^{2+}, Sr^{2+} and Ca^{2+} solutions, respectively, and half-maximal $I_{\omega CgTX}$ was found at −10, −6 and −2 mV. Note that rapid inactivation was only seen in Ca^{2+} solution, indicating

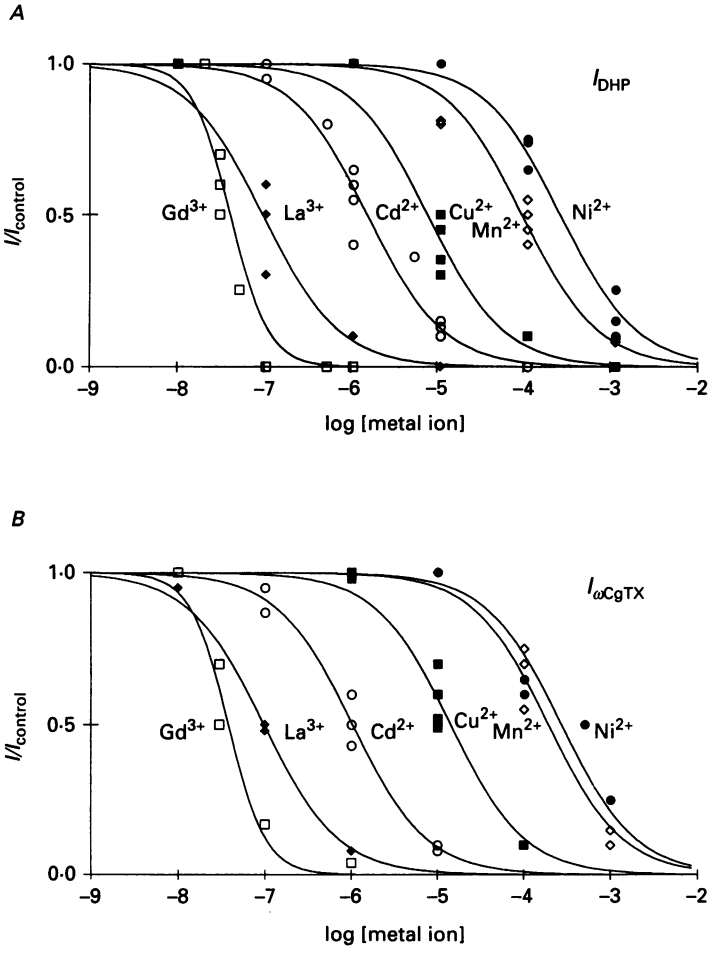

Fig. 10. Blocking of I_{DHP} (*A*) and $I_{\omega CgTX}$ (*B*) by metal ions. The two I_{HVA}s were pharmacologically separated and evoked at 20 mV in the Ca^{2+} solution. Metal ions of different concentrations were sequentially applied. Amplitudes of currents before the application of metal ions was taken as 1. Each point represents a value obtained from one experiment. Gd^{3+} (□), La^{3+} (◆), Cd^{2+} (○), Cu^{2+} (■), Mn^{2+} (◇) and Ni^{2+} (●) were examined. The dose–inhibition curves were fitted with equations: $I = 1/(1+[\text{metal}]^2/K_i^2)$ for Gd^{3+} and $I = 1/(1+[\text{metal}]/K_i)$ for other metals. K_i values are given in the text.

that Ca^{2+}-dependent inactivation of both I_{DHP} and $I_{\omega CgTX}$ is very selective for Ca^{2+} in this cell.

Metal ion block of I_{DHP} and $I_{\omega CgTX}$

Although I_{LVA} and I_{HVA} can be distinguished by their differential block by metal ions such as Ni^{2+} and Cd^{2+} (Tsunoo *et al.* 1986), the two I_{HVA}s did not show substantial difference in their sensitivity to metal ions. Dose–inhibition curves obtained in Fig. 10 give concentrations for half-maximal block (K_i) as 39 nM for Gd^{3+}, 92 nM for La^{3+}, 1·4 μM for Cd^{2+}, 7·1 μM for Cu^{2+}, 85 μM for Mn^{2+}, and 230 μM for Ni^{2+} for I_{DHP}. For $I_{\omega CgTX}$, these values were similar: 38 nM (Gd^{3+}), 98 nM (La^{3+}), 1·0 μM (Cd^{2+}), 14 μM (Cu^{2+}), 190 μM (Mn^{2+}) and 270 μM (Ni^{2+}). The blocking effects of all metal ions except Gd^{3+} developed immediately and were almost completely reversible. The effect of Gd^{3+} was slow to develop, particularly at low concentrations (< 1 μM) and removal of the effect was always incomplete, suggesting that Gd^{3+} permeated the plasma membrane and acted from the inside of the cells.

Docherty (1988) reported that Gd^{3+} blocked only the inactivating I_{HVA} in the same cell line; a half-effective dose for the inactivating current was about 1 μM and the sustained current was not affected even at 50 μM. In addition, in his hands, the effect of Gd^{3+} developed rapidly and quickly washed out. The origin of this discrepancy is not known. However, the two experiments were done in considerably different ionic environments: in particular, (1) we used 10 mM-HEPES for pH buffer, while he used 22·6 mM-bicarbonate and gassed with 5% CO_2, (2) we used 10 mM-Ba^{2+} as charge carrier, while he used 2·5 mM-Ca^{2+} as charge carrier. It can be speculated that bicarbonate buffer precipitated the metal ion and/or converted it to different ionic forms, which are impermeable to plasma membranes. In Ca^{2+} solution, the block of I_{HVA} by Gd^{3+} might be seen as preferential reduction of inactivating component of I_{HVA} (N-current), since inactivation of I_{HVA} is mainly Ca^{2+} dependent.

DHP sensitivity of I_{DHP}

The actions of DHP compounds on I_{DHP} were quantitatively examined. In the experiment shown in Fig. 11, nifedipine reduced the current to 20% of control, whereas Bay K 8644 augmented the current to 220% of control level. Bay K 8644 also shifted the I–V curve in the hyperpolarizing direction by about 10 mV (Fig. 11*C*) and slowed the tail currents (Fig. 11*A*). Effects of both drugs were fully reversible, although reversal took a long time. The half-effective dose of nifedipine required for block was 8·2 nM and the block was maximal at 100 nM (Fig. 11*D*). These actions of DHP compounds are very similar to those already reported in cardiac muscle, although I_{DHP} appears 10 times less sensitive to DHPs than is the DHP-sensitive channel of cardiac muscle (Bean, 1984).

A small fraction (mean = 8%) of the current separated using ωCgTX was not blocked by high concentrations of nifedipine. It is possible, however, that this current flows through the same channels that carry the nifedipine-sensitive current, because the amplitude of the resistant current is proportional to the amplitude of I_{DHP}. This resistant current may be the counterpart of the DHP-sensitive current of cardiac muscle at hyperpolarized V_h, which is not completely blocked by DHP antagonists (Bean, 1984; Sanguinetti & Kass, 1984).

ωCgTX-sensitivity of I_{DHP} and $I_{\omega CgTX}$

The effect of ωCgTX on $I_{\omega CgTX}$ was quantitatively studied in 10 mM-Ba^{2+} solution containing nifedipine. Figure 12 shows the time course of development of block by ωCgTX. The rate of current block depended upon toxin concentration, and could be

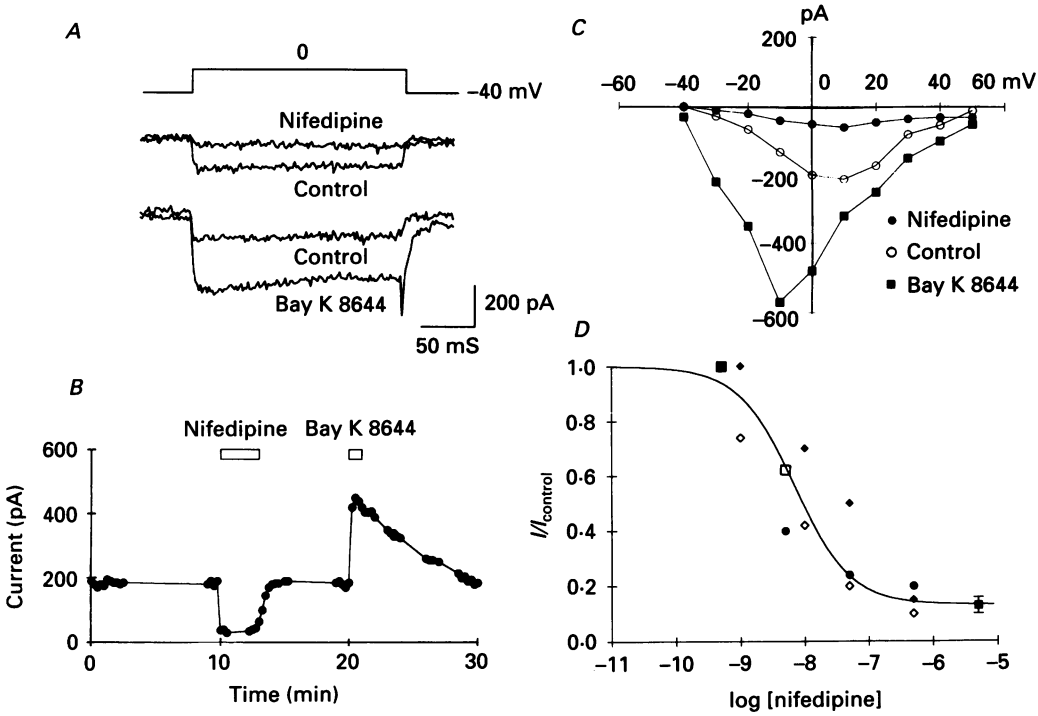

Fig. 11. Effects of dihydropyridine compounds on the I_{DHP}. The I_{DHP} was pharmacologically separated and measured using the perforated patch method in Ba^{2+} solution (*A–C*). *A*, superimposed current traces before and during application of nifedipine (5 μM, upper traces) and Bay K 8644 (5 μM, lower traces). A small inward holding current appeared with Bay K 8644. *B*, time course of the effect of nifedipine and Bay K on the I_{DHP} evoked at 0 mV. *C*, *I–V* relationships during control, in the presence of nifedipine and in the presence of Bay K 8644. *D*, dose–inhibition relationship of nifedipine on the I_{DHP}. Different symbols represent data taken from different cells. The data point at 5 μM is a mean ± S.E.M. of twenty-one experiments. A smooth line was drawn according to the equation: $b = k/1 + [\text{nifedipine}]/K_m) + (1 - k)$, where b represents relative amplitude of the current, $K_m = 8{\cdot}2$ nM and $k = 0{\cdot}92$.

described by a single exponential function with time constants of 6, 65 and 605 s, for 10, 1 and 0·1 μM, respectively. This indicates that ωCgTX combines with a single binding site on the channel with a rate constant of about $1{\cdot}7 \times 10^4$ s^{-1} m^{-1}. The rate constant is comparable to the one in chick DRG neurones (2×10^5 s^{-1} M^{-1} in a 2·5 mM-Ba^{2+} solution, Aosaki & Kasai, 1989), considering the fact that toxin binding is inhibited by a high concentrations of Ba^{2+}, such as were used here (Cruz & Olivera, 1986; Abe & Saisu, 1987). No recovery was detected up to 1 h after wash-out of the drug. This indicates a very high affinity constant and is consistent with ωCgTX

binding studies (Cruz & Olivera, 1986; Abe & Saisu, 1987). In most experiments, we used very high concentrations of the toxin,in order to block the current quickly.

ωCgTX reversibly blocked I_{DHP} in a small population of the cells. Figure 12*B* shows an extreme case where 50% of I_{HVA} was reversibly affected by ωCgTX. The

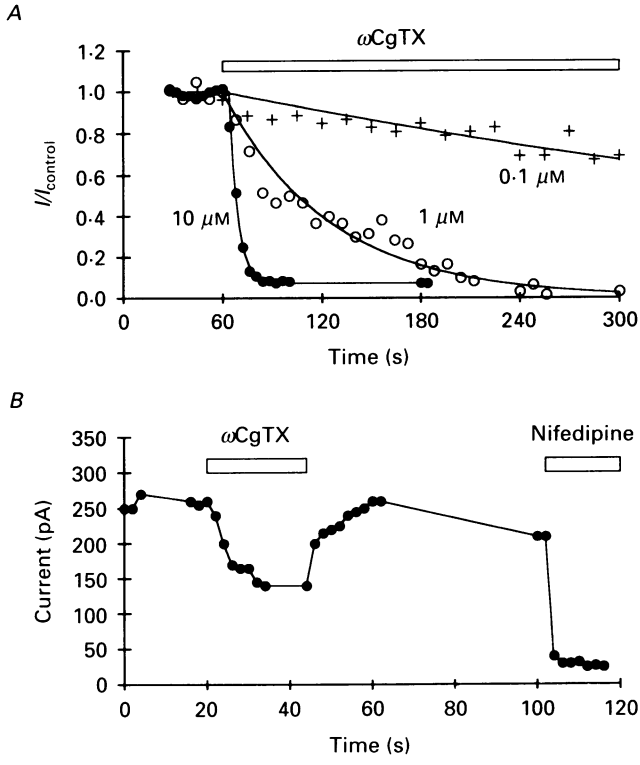

Fig. 12. Effects of ωCgTX on $I_{\omega CgTX}$ and I_{DHP}. The two I_{HVA}s were pharmacologically separated and evoked at 0 mV in Ba^{2+} solution. *A*, time courses of the block of $I_{\omega CgTX}$ by ωCgTX at three different concentrations (0·1, 1 and 10 μM). Smooth lines were drawn according to an equation: $b = k\exp(-\alpha[\omega CgTX]t)+(1-k)$, where b represents relative amplitude of the current, k amount of block and α an association rate of constant. The values were $k = 1$ and $\alpha = 1{\cdot}6 \times 10^4\ s^{-1}$ at 0·1 μM, $k = 1$ and $\alpha = 1{\cdot}5 \times 10^4\ s^{-1}$ at 1 μM, and $k = 0{\cdot}92$ and $\alpha = 2 \times 10^4\ s^{-1}$ at 10 μM. *B*, reversible effect of ωCgTX (5 μM) on I_{DHP}, which was mostly eliminated by nifedipine (5 μM).

I_{HVA} of this cell was mainly I_{DHP} since it was blocked by 92% by nifedipine. This indicates that part of I_{DHP} is reversibly blocked by ωCgTX, as is the case in chick DRG neurones (Kasai *et al.* 1987). However, reversible block of I_{DHP} by ωCgTX was present in only a very small population (5%) of NG-108 cells and even in these sensitive cells the amount of current reduction was very small (mean = 10%).

Effect of N-ethylmaleimide on I_{DHP} and $I_{\omega CgTX}$

N-Ethylmaleimide is an agent that alkylates sulphydryl groups. We found that NEM specifically augmented I_{DHP}, with 0·1 mM-NEM gradually increasing current by up to 30% (at 0 mV). The facilitatory effect of NEM was sustained if application

of NEM was stopped after 60 s, while longer exposure to NEM tended to reduce the current. The facilitatory effect of NEM can be described as a hyperpolarizing shift of the *I–V* curve (Fig. 13*C*). Unlike Bay K 8644, NEM did not increase currents evoked at stronger depolarizations or slow tail currents (Fig. 13*D*). At higher NEM

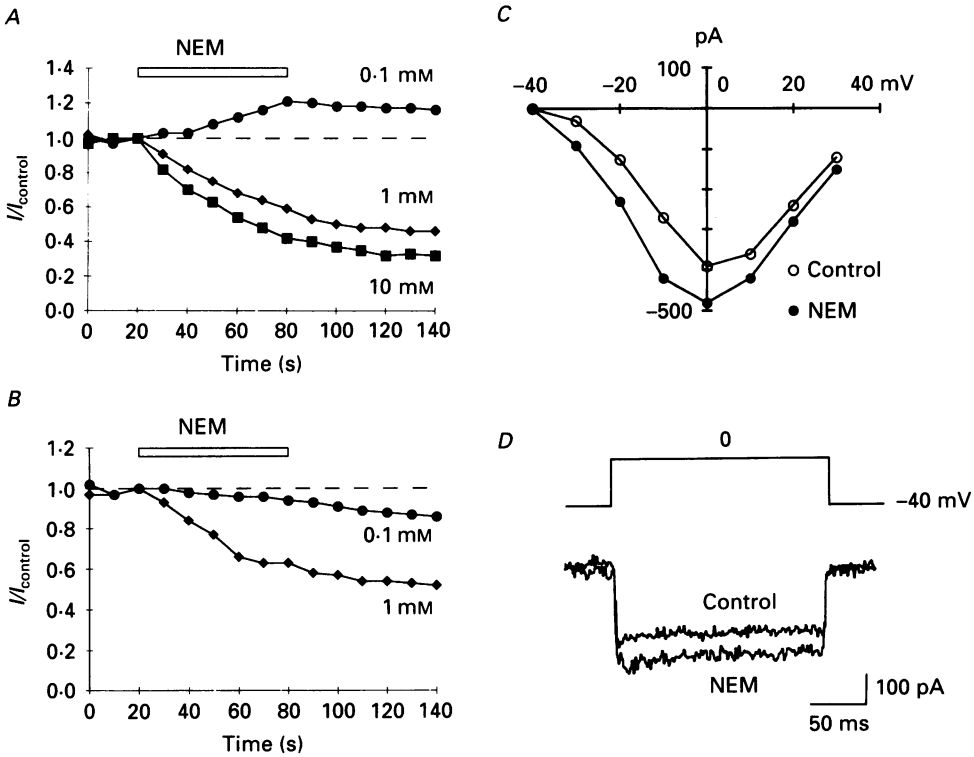

Fig. 13. Effects of *N*-ethylmaleimide (NEM) on I_{DHP} and $I_{\omega CgTX}$. The two I_{HVA}s were pharmacologically separated and evoked at 0 mV in Ba^{2+} solution. *A* and *B*, time courses of actions of NEM at different concentrations (0·1, 1 and 10 mM) on I_{DHP} (*A*) and $I_{\omega CgTX}$ (*B*). *C*, *I–V* relationship of I_{DHP} before and after a short treatment (30 s) of NEM (0·1 mM). *D*, superimposed current traces evoked at 0 mV before and after the short treatment with NEM.

concentrations, I_{DHP} was irreversibly reduced (Fig. 13*A*). In contrast, NEM reduced $I_{\omega CgTX}$ at any concentration (Fig. 13*B*). These data indicate that the DHP-sensitive channel has a cysteine moiety that reacts rapidly with NEM and that affects the gating of the channel. Similar facilitatory effects of NEM on cardiac DHP-sensitive channels have recently been reported (Nakajima, Irisawa & Giles, 1990).

Developmental changes in I_{LVA}, I_{DHP} and $I_{\omega CgTX}$

All of the experiments shown above were made in cells differentiated with dibutyryl cyclic AMP or with prostaglandin E_1 and theophylline. Some small I_{HVA} was sometimes recorded from undifferentiated cells, and quite large I_{HVA} was developed already after a mild differentiation (1–2 days). The I_{HVA} in these early days of differentiation was mostly I_{DHP} (Fig. 14). It was not until 3 days after

differentiation that $I_{\omega CgTX}$ was fully developed (Fig. 14). Thus, I_{DHP} developed earlier than $I_{\omega CgTX}$ during the course of dibutyryl cyclic AMP treatment. This parallels a report showing that large $I_{\omega CgTX}$ was developed after NGF treatment in PC12 cells (Plummer *et al.* 1989). The amount of I_{LVA} did not change appreciably during development (Fig. 14).

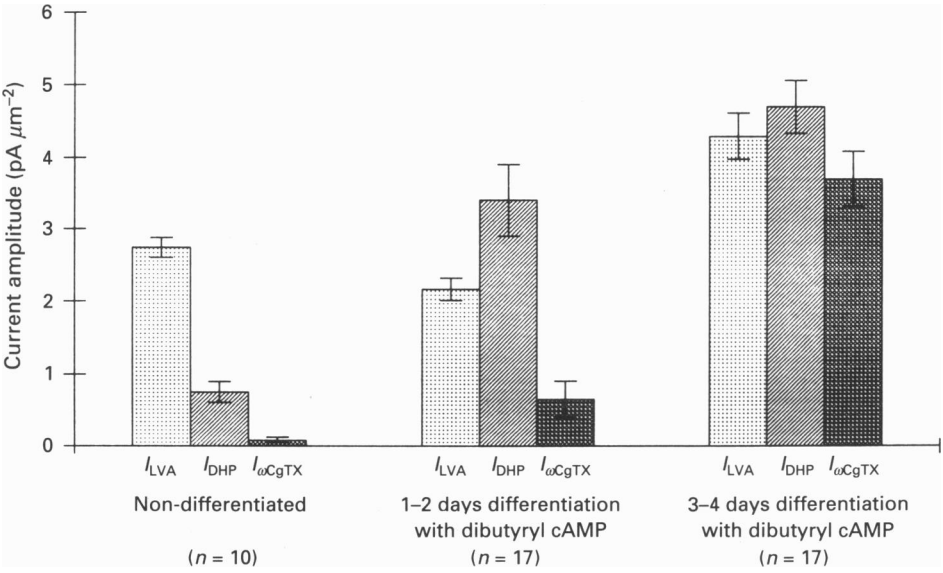

Fig. 14. Development of the three Ca^{2+} channels of NG108–15 cells during differentiation induced by dibutyryl cyclic AMP. The amplitude of I_{LVA} was measured at a peak current evoked at −30 mV from V_h of −60 mV and that of I_{HVA} at a peak evoked at 20 mV from V_h of −40 mV. I_{DHP} and $I_{\omega CgTX}$ were identified either with nifedipine or ωCgTX. The amplitudes of the current were normalized with respect to membrane capacitance. Bars show S.E.M.

DISCUSSION

Pharmacological classes of vertebrate neuronal Ca^{2+} channels

We have examined the properties of I_{HVA} in the neuroblastoma–glioma hybrid cell line, NG108–15. I_{HVA} has been classified into two components based on sensitivity to dihydropyridine (DHP) compounds and ω-conotoxin GVIA (ωCgTX): one component (I_{DHP}) is selectively and reversibly blocked with the DHP antagonist, nifedipine (K_d = 8 nM), while the other ($I_{\omega CgTX}$) is selectively blocked by ωCgTX in an irreversible manner. These findings indicate that the two I_{HVA}s are carried by different Ca^{2+} channel molecules. This type of heterogeneity of Ca^{2+} channels is likely to be general in vertebrate species, since the same pharmacological distinction has been found in neuronal cells of chick (Kasai *et al.* 1987; Aosaki & Kasai, 1989), rat (Plummer *et al.* 1989; Regan *et al.* 1991) and human (Carbone *et al.* 1990).

The two I_{HVA}s studied here do not fit into the classification scheme proposed for chick DRG neurones by Tsien *et al.* (1988). Although both I_{DHP} and 'L-type current' are blocked by DHP antagonists, I_{DHP} is resistant to ωCgTX while 'L-type current' is not (Fox *et al.* 1987*a*). In addition, I_{DHP} shows prominent inactivation in Ca^{2+}

solution, while 'L-type current' is not (Tsien *et al.* 1988). Although both $I_{\omega CgTX}$ and 'N-type current' were blocked by ωCgTX, $I_{\omega CgTX}$ shows small inactivation, unlike 'N-type' current. Indeed, I_{WCgTX} was recorded at a depolarized holding potential (V_h) which should completely inactivate 'N-type' current (Fox *et al.* 1987*a*).

Many studies have used inactivation properties to separate I_{HVA} into two components (see for example, Fox *et al.* 1987*a*; Kostyuk, Shuba & Savchenko, 1988; Docherty, 1988). None of these studies systematically investigated the effects of DHP antagonists on the inactivation-resistant component of I_{HVA}. Moreover, ωCgTX often irreversibly affected both current components. It is therefore evident that 'L-type' and 'N-type' currents separated by inactivation are not necessarily correlated with the currents separated on the basis of their pharmacological properties. For example, I_{HVA} of the NG108–15 cell was classified into 'L-type' and 'N-type' in a Ca^{2+} solution (Docherty, 1988). However, in our hands, the inactivating 'N-type' current is mainly a component of I_{DHP} that is inactivated by a Ca^{2+}-dependent mechanism (Fig. 8*A*). As a result of the differences in the definitions, properties of 'L-type' and 'N-type' currents reported in the earlier studies (Tsien *et al.* 1988) are essentially deviated from those of I_{DHP} and $I_{\omega CgTX}$ in their major properties: activation, inactivation and modulation by a GTP-binding protein (see below and Kasai, 1992).

Non-selective effects of ωCgTX

ωCgTX affects Ca^{2+} channel currents other than $I_{\omega CgTX}$ in a partial and reversible way in NG108–15 cells. Partial and reversible block of I_{DHP} has also been reported for rat retinal ganglion cells (Karschin & Lipton, 1989) and chick DRG neurones (Kasai *et al.* 1987). In chick DRG neurones, DHP-sensitive single-channel currents were either reversibly blocked with ωCgTX or insensitive to the toxin (Aosaki & Kasai, 1989). In muscle cells, no effect of ωCgTX on I_{DHP} has been detected (McCleskey, Fox, Feldman, Cruz, Olivera & Tsien, 1987). It is likely that a subtype of DHP-sensitive channel is reversibly blocked by ωCgTX. Plummer *et al.* (1989) and Jones & Marks (1989) have also reported a partial and reversible effect of ωCgTX on I_{HVA}. However, the nature of the current was not clear, since they did not examine sensitivities to DHPs. I_{LVA} was also reversibly blocked by ωCgTX in chick DRG neurones (McClesky *et al.* 1987; Kasai & Aosaki, 1987) and in NG108–15 cells (H. Kasai unpublished observation).

The fact that ωCgTX blocks I_{DHP} and I_{LVA} as well as $I_{\omega CgTX}$ with similar time courses (Fig. 12*B*; Aosaki & Kasai, 1989) indicates that the specificity of the action of ωCgTX on $I_{\omega CgTX}$ is ascribed to its unmeasurably low dissociation rate, whereas the association rates are similar among these channels (Aosaki & Kasai, 1989). It could be speculated that ωCgTX blocks ωCgTX-sensitive channels in such a way that the toxin first combines with a site common to many Ca^{2+} channels, followed by a transition to a specific binding site associated with a conformational change in the toxin. Two binding sites with different affinities for ωCgTX have been found in rat brain (Abe, Hayakawa, Yamaguchi, Morita, Saisu & Mitsui, 1986).

Non-specific effects of DHP compounds

DHP compounds are known to have blocking effects on other molecules, when used at high concentrations. For instance, block of I_{LVA} has been reported in hippocampal pyramidal cells (Akaike, Kostyuk & Osipchuk, 1989) and in NG108–15 cells (H. Kasai, unpublished observation). Block of $I_{\omega CgTX}$ by a DHP agonist was reported in chick DRG neurones (Boll & Lux, 1985; Kasai *et al.* 1987; Aosaki & Kasai, 1989) and frog sympathetic neurones (Jones & Jacobs, 1990). Furthermore, DHPs also block Na^+ and K^+ currents (Jones & Jacobs, 1990) and agonist binding to muscarinic and α-adrenergic receptors (Thayer, Welcome, Chhabra & Fairhurst, 1985). These effects occur at DHP concentrations of a few micromolar, which is more than a hundred times larger than required for block of I_{DHP} in the NG108 cell.

Activation gating

In order to compare the activation gating of the two I_{HVA}s, the data shown in Figs 4 and 5 were fitted with the Hodgkin–Huxley model and the parameters (n_∞ and τ) describing voltage dependence and kinetics were obtained (Fig. 15). Four major differences were found. (1) n_∞ takes its half-maximal value at a potential 16 mV more hyperpolarized in I_{DHP} than in $I_{\omega CgTX}$. (ii) The slope of n_∞ is less steep in I_{DHP} than in $I_{\omega CgTX}$. (iii) τ is two times smaller in I_{DHP} than in $I_{\omega CgTX}$. (iv) τ reaches its maximum at a potential 20 mV more hyperpolarized in I_{DHP} than in $I_{\omega CgTX}$.

It is important to note that all these differences cause I_{DHP} to be activated at smaller depolarizations than for activation of $I_{\omega CgTX}$. In addition, these differences are amplified by the fact that I_{DHP} can be activated at a potential which is subthreshold for the activation of voltage-dependent K^+ currents (Fig. 6). These observations suggest that I_{DHP} is more likely involved in generation of Ca^{2+} spikes and Ca^{2+} plateau potentials. Indeed, DHP compounds altered the threshold for Ca^{2+} spike generation in rat hippocampal pyramidal cells (Gaehwiler & Brown, 1987). On the other hand, $I_{\omega CgTX}$ is more specialized in Ca^{2+} influx triggered by Na^+ spikes. This feature of $I_{\omega CgTX}$ seems more appropriate for a Ca^{2+} channel that regulates neurotransmitter release (see below), since Ca^{2+} spikes should not be triggered by fluctuations of membrane potential at presynaptic terminals.

The difference in the activation gating of I_{DHP} and $I_{\omega CgTX}$ may be common in vertebrate species. Two of the properties listed above, (i) and (ii), have also been noted in chick DRG neurones (Kasai *et al.* 1987; Aosaki & Kasai, 1989), in rat primary neurones (Regan *et al.* 1991) and in human neuroblastoma cell (Carbone *et al.* 1990). On the other hand, it has been surmised (Tsien *et al.* 1988) that the 'L-type current' had higher activation threshold than the 'N-type current'. This obvious discrepancy is due to differences in the criteria used for current separation.

Mechanisms of inactivation

The properties of the inactivation of I_{DHP} are similar to those reported for the DHP-sensitive current of muscle (Lee, Marban & Tsien, 1985). Those channels are equipped with two mechanisms of inactivation: one voltage dependent and the other Ca^{2+} dependent. The latter is characterized by (1) relief by strong depolarization, (2) selectivity toward Ca^{2+} over Sr^{2+} and Ba^{2+}, (3) attenuation of inactivation by

intracellular buffers (Chad, 1989). We have shown that inactivation of I_{DHP} in Ca^{2+} solution fulfilled the first two criteria.

The $I_{\omega CgTX}$ was also equipped with both inactivation mechanisms, although the voltage-dependent inactivation was small (Figs 1 and 7). The Ca^{2+}-dependent

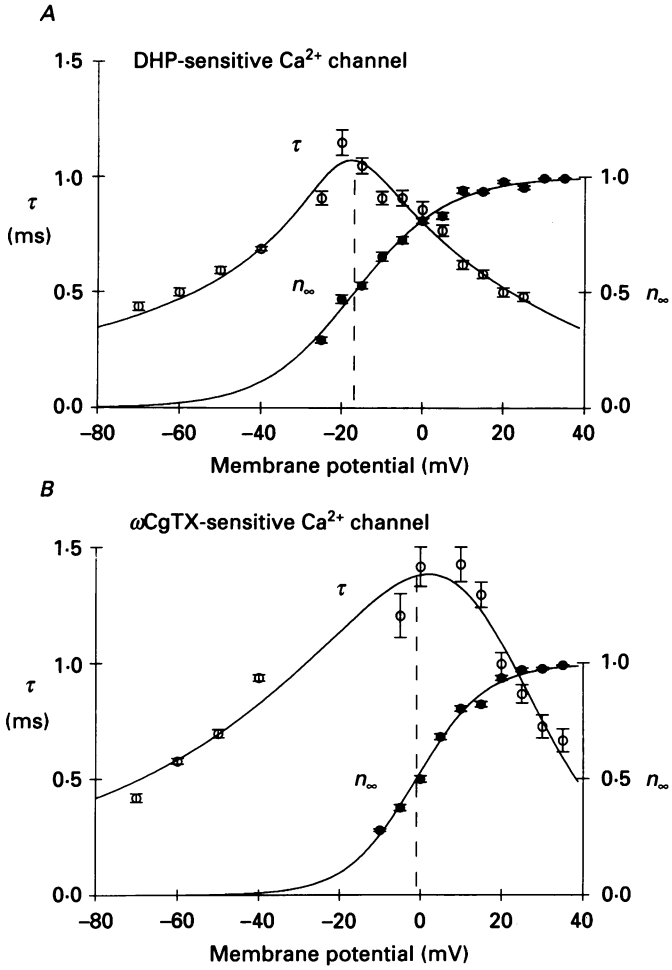

Fig. 15. Voltage dependence of the activation gating of DHP-sensitive (*A*) and ωCgTX-sensitive (*B*) Ca^{2+} channels. The data were analysed using a m^2 Hodgkin–Huxley model. Values of τ (○) at potentials smaller than −30 mV were obtained from tail currents (Fig. 4*C* (and those at potentials larger than −30 mV from the activation time courses (Fig. 4*A*). Values for the activation (●) were obtained from the activation curves (Fig. 5). Smooth lines were drawn according to equations: $\tau = 1/(\alpha+\beta)$, $n_\infty = \beta/(\alpha+\beta)$, $\alpha = C(V-V_m)/[\exp\{(V-V_m)/k\}-1]$ and $\beta = C'\exp(V/k')$, where V represents membrane potential, α, closing rate constant, and β, opening rate constant. The parameters were $V_m = -8{\cdot}124$, $k = 9{\cdot}005$, $k' = 31{\cdot}4$, $C = 0{\cdot}0398$ and $C' = 0{\cdot}99$ for I_{DHP} and $V_m = -17{\cdot}19$, $k = 15{\cdot}22$, $k' = 23{\cdot}82$, $C = 0{\cdot}03856$ and $C' = 0{\cdot}3842$ for $I_{\omega CgTX}$.

inactivation of $I_{\omega CgTX}$ appears to be different from that of I_{DHP}, even though both were studied in the same neuronal cells. Ca^{2+}-dependent inactivation of $I_{\omega CgTX}$ is slower to develop and recover. Inactivation of $I_{\omega CgTX}$ in chick DRG neurones is more prominent and does not depend so much on divalent species (Kasai & Aosaki, 1988). Apparently, there is diversity in Ca^{2+}-dependent inactivation mechanisms.

In the case of I_{DHP}, we found a pronounced anomaly in the time course of the Ca^{2+}-dependent inactivation (Fig. 8). A similar anomaly in Ca^{2+}-dependent inactivation was found for Ca^{2+} currents of a molluscan neurone and was interpreted to indicate that the inactivation was induced by a local rise in $[Ca^{2+}]_i$ beneath the internal mouth of each single channel and that the rise in Ca^{2+} was higher at hyperpolarized membrane potentials where the driving force for Ca^{2+} influx was larger (Chad & Eckert, 1984). A similar anomaly was reported for I_{DHP} of an endocrine cell (Plant, 1988), while it was not seen in I_{CgTX} of NG108–15 (Fig. 8) or chick DRG neurones (Kasai & Aosaki, 1988; Aosaki & Kasai, 1989). This might be related to the fact that ωCgTX-sensitive channels are often extremely clustered (Fox *et al.* 1987*b*; Aosaki & Kasai, 1989), and that the local rise in Ca^{2+} parallels with amplitude of macroscopic $I_{\omega CgTX}$ rather than that of single $I_{\omega CgTX}$ (Augustine, Charlton & Smith, 1987).

Localization of the channels

The two HVA currents are unevenly distributed in neuronal membranes. First, they are differently distributed among types of neurones. I_{HVA} of rat retinal ganglion cells is mostly composed of I_{DHP} (Karschin & Lipton, 1989), whereas I_{HVA} of the chick DRG neurones is predominantly $I_{\omega CgTX}$ (Aosaki & Kasai, 1989). I_{HVA} of cerebellar Purkinje cells has little $I_{\omega CgTX}$ (see below). Secondly, even within a single cell type the relative abundance of the two I_{HVA} components varies widely (Aosaki & Kasai, 1989; this study). The functional significance of this variability has not been explored.

The two HVA Ca^{2+} channels seem to be segregated even within a single neurone. In most synapses, neurotransmitter release is partly blocked by ωCgTX but not by DHP antagonists (Kerr & Yoshikami, 1984; Kamiya, Sawada & Yamamoto, 1988; Hirning, Fox, McClesky, Olivera, Thayer, Miller & Tsien, 1988; but see Lindgren & Moore, 1989). This indicates that the ωCgTX-sensitive channels are more often localized in presynaptic release sites than the DHP-sensitive channels. Two properties of the ωCgTX-sensitive channel may make it more suitable than the DHP-sensitive channel may make it more suitable than the DHP-sensitive channel for triggering neurotransmitter release. Firstly, its higher activation threshold prevents autonomous firing of the presynaptic terminal (see above). Secondly, it can be inhibited by neurotransmitters (Kasai & Aosaki, 1989; Kasai, 1992), which is likely to be an important mechanism for presynaptic inhibition (Lipscombe, Kongsamut & Tsien, 1989). Preferential localization of DHP-sensitive Ca^{2+} channels in proximal dendrites of CA1 pyramidal cells have been reported (Westenbroek, Ahlijanian & Catterall, 1990). Those DHP-sensitive channels may be used in generating dendritic Ca^{2+} spikes.

Biochemical entities of vertebrate Ca^{2+} channels

Our pharmacological classification of two types of HVA currents is consistent with recent biochemical studies. Firstly, monoclonal antibodies which immunoprecipitated most of brain DHP binding sites did not significantly precipitate ωCgTX binding sites (Abe *et al.* 1989; Westenbroek *et al.* 1990). Secondly, in chick and rat

TABLE 2. Classes of Ca^{2+} channels in vertebrate neurones

	LVA	DHP sensitive	ωCgTX sensitive	Others
Dihydropyridine (DHP)	—	+	—	—
ω-Conotoxin GVIA (ωCTX)	—	—	+	—
Single-channel conductance (pS)	8	25	13	~
Activation threshold (mV)	−50	−30	−20	~
Inactivation mechanisms	Voltage dependent	Voltage and Ca^{2+} dependent		~
Inhibition by a G-protein	±	±	+	~

brain, ωCgTX was cross-linked to two proteins (Abe & Saisu, 1987; Cruz, Imperial, Johnson & Olivera, 1987) with molecular weights significantly larger than that of DHP receptors (MacKenna, Koch, Slish & Schwartz, 1990).

The functional differences between the two classes of channels imply structural dissimilarities between the two channels. Those are the functional domains for (1) DHP binding, (2) ωCgTX binding, (3) alkylation by NEM, (4) activation gating, (5) inactivation gating, (6) Ca^{2+}-dependent inactivation, (7) Ca^{2+} carrying capacity, and (8) the regulation by a GTP-binding protein. In spite of differences in many parts of the channels, the structure essential for ion selectivity may be similar, since the two HVA Ca^{2+} channels are very similar in their selectivities among different divalent cations and in blocking action by different metal ions.

Functional classes of vertebrate neuronal Ca^{2+} channels

The classes of HVA Ca^{2+} channels show pronounced differences in both development and function. The major characteristics of the two channels appear to be conserved in neurones of different species. It is therefore reasonable to think that the ωCgTX-sensitive and DHP-sensitive channels belong to separate functional species. Major properties of the three Ca^{2+} channels are listed in Table 2.

Most of the I_{HVA} in NG108–15 cells and in chick DRG neurones is either sensitive to DHP or sensitive to ωCgTX. In other mammalian neurones, however, a substantial component of I_{HVA} is resistant to both antagonists (Plummer *et al.* 1989). The resistant I_{HVA} is differently distributed among different acutely dissociated central and peripheral neurones (Regan *et al.* 1991). One extreme example is the cerebellar Purkinje cell, where most of the current falls into this class (Llinás, Sugimori, Lin & Cherlsey, 1988; Lin, Rudy & Llinás, 1990). Presumably there must be at least one additional pharmacological class of HVA Ca^{2+} channel. On the other hand, it is known that a single point mutation can eliminate TTX sensitivity from a Na^+ channel without affecting its gating properties (Noda, Suzuki, Numa & Stühmer, 1989).

Recently, rat brain cDNAs homologous to the α_1-subunit of muscle DHP-sensitive Ca^{2+} channels were cloned and grouped into four major classes (Snutch, Leonard, Gilbert & Lester, 1990). It is of importance to know how these biochemical classifications correlate with those deduced from functional and pharmacological evidence. Better characterization of neuronal Ca^{2+} channels, based on a precise pharmacology, is necessary to clarify functional and molecular properties of brain Ca^{2+} channels. NG108–15 cells represent a good system to both survey actions of various drugs on specific classes of Ca^{2+} channel currents and to elucidate their molecular characteristics.

The authors thank Bernd Hamprecht for kindly supplying the neuroblastoma–glioma cell line. We are also grateful to Monika Papke and Michale Pilot for preparing the cultured cells, George J. Augustine for improving the manuscript, Walter Sthümer, and Reinhold Penner and Michael Pusche for computer programming. This work was supported by an Alexander von Humboldt fellowship to H.K. and by a DFG grant to E.N.

REFERENCES

ABE, T., HAYAKAWA, N., YAMAGUCHI, T., MORITA, T., SAISU, H. & MITSUI, H. (1989). The high-affinity receptor for ω-conotoxin in brain differs from the dihydropyridine receptor. *Society for Neuroscience Abstracts* **15**, 355.

ABE, T. & SAISU, H. (1987). Identification of the receptor for ω-conotoxin in brain. *Journal of Biological Chemistry* **262**, 9877–9882.

AKAIKE, N., KOSTYUK, P. G. & OSIPCHUK, Y. V. (1989). Dihydropyridine-sensitive low-threshold calcium channels in isolated rat hypothalamic neurones. *Journal of Physiology* **412**, 181–195.

AOSAKI, T. & KASAI, H. (1989). Characterization of two kinds of high-voltage-activated Ca-channel currents in chick sensory neurons. *Pflügers Archiv* **414**, 150–156.

ARMSTRONG, C. M. & BEZANILLA, F. (1977). Inactivation of the sodium channel. II. Gating current experiments. *Journal of General Physiology* **70**, 567–590.

AUGUSTINE, G. J., CHARLTON, M. P. & SMITH, S. J. (1987). Calcium action is synaptic transmitter release. *Annual Review of Neuroscience* **10**, 633–693.

BEAN, B. P. (1984). Nitrendipine block of cardiac calcium channels: high-affinity binding to the inactivated state. *Proceedings of the National Academy of Sciences of the USA* **81**, 6388–6392.

BEAN, B. P. (1989). Classes of calcium channels in vertebrate cells. *Annual Review of Physiology* **51**, 367–384.

BOLL, W. & LUX, H. D. (1985). Action of organic antagonists on neuronal calcium currents. *Neuroscience Letters* **56**, 335–339.

CARBONE, E. & LUX, D. H. (1987). Single low-voltage-activated calcium channels in chick and rat sensory neurones. *Journal of Physiology* **386**, 571–601.

CARBONE, E., SHER, E. & CLEMENTI, F. (1990). Ca currents in human neuroblastoma IMR32 cells: kinetics, permeability and pharmacology. *Pflügers Archiv* **416**, 170–179.

CARBONE, E. & SWANDULLA, D. (1989). Neuronal calcium channels: kinetics, blockade and modulation. *Progress in Biophysics and Molecular Biology* **54**, 31–58.

CHAD, J. (1989). Inactivation of calcium channels. *Comparative Biochemistry and Physiology* **93A**, 95–105.

CHAD, J. & ECKERT, R. (1984). Calcium domains associated with individual channels can account for anomalous voltage relations of Ca-dependent responses. *Biophysical Journal* **45**, 993–999.

CRUZ, L. J., IMPERIAL, J. S., JOHNSON, D. S. & OLIVERA, B. M. (1987). Crosslinking by ^{125}I-ω-conotoxin: Evidence suggesting multiple neuronal calcium channel subtypes. *Society for Neuroscience Abstracts* **13**, 1011.

CRUZ, L. J. & OLIVERA, B. M. (1986). Calcium channel antagonists. *Journal of Biological Chemistry* **261**, 6230–6233.

DOCHERTY, R. J. (1988). Gadolinium selectively blocks a component of calcium current in rodent neuroblastoma × glioma hybrid NG108–15 cells. *Journal of Physiology* **398**, 33–47.

FENWICK, E. M., MARTY, A. & NEHER, E. (1982). Sodium and calcium channels in bovine chromaffin cells. *Journal of Physiology* **331**, 599–635.

FOX, A. P., NOWYCKY, M. C. & TSIEN, R. W. (1987*a*). Kinetic and pharmacological properties distinguishing three types of calcium currents in chick sensory neurones. *Journal of Physiology* **394**, 149–172.

FOX, A. P., NOWYCKY, M. C. & TSIEN, R. W. (1987*b*). Single-channel recordings of three types of calcium channels in chick sensory neurones. *Journal of Physiology* **394**, 173–200.

GAEHWILER, B. H. & BROWN, D. A. (1987). Effects of dihydropyridines on calcium currents in CA3 pyramidal cells in slice cultures of rat hippocampus. *Neuroscience* **20**, 731–738.

GRAY, W. R., OLIVERA, B. M. & CRUZ, L. J. (1988). Peptide toxins from venomous *Conus* snails. *Annual Review of Biochemistry* **57**, 665–700.

HAMILL, O. P., MARTY, A., NEHER, E., SAKMANN, B. & SIGWORTH, F. (1981). Improved patch-clamp techniques for high-resolution current recording from cells and cell-free membrane patches. *Pflügers Archiv* **391**, 85–100.

HAMPRECHT, B. (1977). Structural, electrophysiological, biochemical, and pharmacological properties of neuroblastoma–glioma cell hybrids in cell culture. *International Review of Cytology* **49**, 99–170.

HESS, P. (1990). Calcium channels in vertebrate cells. *Annual Review in Neuroscience* **13**, 337–356.

HIRNING, L. D., FOX, A. P., MCCLESKEY, E. W., OLIVERA, B. M., THAYER, S. A., MILLER, R. J. & TSIEN, R. W. (1988). Dominant role of N-type Ca channels in evoked release of norepinephrine from sympathetic neurons. *Science* **239**, 57–61.

HODGKIN, A. L. & HUXLEY, A. F. (1952). A quantitative description of membrane current and its application to conduction and excitation in nerve. *Journal of Physiology* **117**, 500–544.

HORN, R. & MARTY, A. (1988). Muscarinic activation of ionic currents measured by a new whole-cell recording method. *Journal of General Physiology* **92**, 145–159.

HOSHI, T., ROTHLEIN, J. & SMITH, S. J. (1984). Facilitation of Ca^{2+}-channel currents in bovine adrenal chromaffin cells. *Proceedings of the National Academy of Sciences of the USA* 81, 5871–5875.

JONES, S. W. & JACOBS, L. S. (1990). Dihydropyridine actions on calcium currents of frog sympathetic neurons. *Journal of Neuroscience* **10**, 2261–2267.

JONES, S. W. & MARKS, T. N. (1989). Calcium currents in bullfrog sympathetic neurons. *Journal of General Physiology* **94**, 151–167.

KAMIYA, H., SAWADA, S. & YAMAMOTO, C. (1988). Synthetic ω-conotoxin blocks synaptic transmission in the hippocampus in vitro. *Neuroscience Letters* **91**, 84–88.

KARSCHIN, A. & LIPTON, S. A. (1989). Calcium channels in solitary retinal ganglion cells from post-natal rat. *Journal of Physiology* **418**, 379–396.

KASAI, H. (1987). Presynaptic Ca-antagonist ω-conotoxin irreversibly blocks N-type Ca-channels in chick sensory neurons. *Biophysical Journal* **51**, 31a.

KASAI, H. (1989). Three components of Ca-channel currents and their modulation by a GTP-binding protein. *Society for Neuroscience Abstracts* **15**, 1149.

KASAI, H. (1992). Voltage- and time-dependent inhibition of neuronal calcium channels by a GTP-binding protein in a mammalian cell line. *Journal of Physiology* **448**, 189–209.

KASAI, H., AOSAKI, T. & FUKUDA, J. (1987). Presynaptic Ca-antagonist ω-conotoxin irreversibly blocks N-type Ca-channels in chick sensory neurons. *Neuroscience Research* **4**, 228–235.

KASAI, H. & AOSAKI, T. (1988). Divalent cation dependent inactivation of the high-voltage-activated Ca-channel current in chick sensory neurons. *Pflügers Archiv* **411**, 695–697.

KASAI, H. & AOSAKI, T. (1989). Modulation of Ca-channel current by an adenosine analog mediated by a GTP-binding protein in chick sensory neurons. *Pflügers Archiv* **414**, 145–149.

KERR, L. M. & YOSHIKAMI, D. (1984). A venom peptide with a novel presynaptic blocking action. *Nature* **308**, 282–284.

KOSTYUK, P. G., SHUBA, Y. M. & SAVCHENKO, A. N. (1988). Three types of calcium channels in the membrane of mouse sensory neurons. *Pflügers Archiv* **411**, 661–669.

LEE, K. S. (1987). Potentiation of the calcium-channel currents of internally perfused mammalian heart cells by repetitive depolarization. *Proceedings of the National Academy of Sciences of the USA* **84**, 3941–3945.

LEE, K. S., MARBAN, E. & TSIEN, R. W. (1985). Inactivation of calcium channels in mammalian

heart cells: joint dependence on membrane potential and intracellular calcium. *Journal of Physiology* **364**, 395–411.

LIN, J.-W., RUDY, B. & LLINÁS, R. (1990). Funnel-web spider venom and a toxin fraction block calcium current expressed from rat brain mRNA in Xenopus oocytes. *Proceedings of the National Academy of Sciences of the USA* **87**, 4538–4542.

LINDGREN, C. A. & MOORE, J. W. (1989). Identification of ionic current at presynaptic nerve endings of the lizard. *Journal of Physiology* **414**, 201–222.

LIPSCOMBE, D., KONGSAMUT, S. & TSIEN, R. W. (1989). α-Adrenergic inhibition of sympathetic neurotransmitter release mediated by modulation of N-type calcium-channel gating. *Nature* **340**, 639–642.

LLINÁS, R., SUGIMORI, M., LIN, J.-W. & CHERLSEY, B. (1989). Blocking and isolation of a calcium channel from neurons in mammals and cephalopods utilizing a toxin fraction (FTX) from funnel-web spider poison. *Proceedings of the National Academy of Sciences of the USA* **86**, 1689–1693.

MCCLESKEY, E. W., FOX, A. P., FELDMAN, D. H., CRUZ, L. J., OLIVERA, B. M. & TSIEN, R. W. (1987). ω-Conotoxin: direct and persistent blockade of specific types of calcium channels in neurons but not muscle. *Proceedings of the National Academy of Sciences of the USA* **84**, 4327–4331.

MACKENNA, E., KOCH, W. J., SLISH, D. F. & SCHWARTZ, A. (1990). Toward an understanding of the dihydropyridine-sensitive calcium channel. *Biochemical Pharmacology* **39**, 1145–1150.

MILLER, R. (1984). Are dihydropyridine binding sites voltage sensitive calcium channels? *Life Sciences* **34**, 1205–1221.

NAKAJIMA, T., IRISAWA, H. & GILES, W. (1990). *N*-Ethylmakeimide uncouples muscarinic receptors from acetylcholine-sensitive potassium channels in bullfrog atrium. *Journal of General Physiology* **96**, 887–903.

NARAHASHI, T., TSUNOO, A. & YOSHII, M. (1987). Characterization of two types of calcium channels in mouse neuroblastoma cells. *Journal of Physiology* **383**, 231–249.

NODA, M., SUZUKI, H., NUMA, S. & STÜHMER, W. (1989). A single point mutation confers tetrodotoxin and saxitoxin insensitivity on the sodium channel II. *FEBS Letters* **259**, 213–216.

NOWYCKY, M. C., FOX, A. P. & TSIEN, R. W. (1985). Three types of neuronal calcium channel with different calcium agonist sensitivity. *Nature* **316**, 440–443.

PLANT, T. D. (1988). Properties and calcium-dependent inactivation of calcium currents in cultured mouse pancreatic B-cells. *Journal of Physiology* **404**, 731–747.

PLUMMER, M. R., LOGOTHETIS, D. E. & HESS, P. (1989). Elementary properties and pharmacological sensitivities of calcium channels in mammalian peripheral neurons. *Neuron* **2**, 1453–1463.

REGAN, L. J., SAH, W. Y. & BEAN, B. (1991). Ca^{2+} channels in rat central and peripheral neurons: High-threshold current resistant to dihydropyridine blockers and ω-Conotoxin. *Neuron* **6**, 269–280.

SANGUINETTI, M. C. & KASS, R. C. (1984). Voltage-dependent block of calcium channel current in the calf Purkinje fiber by dihydropyridine Ca-antagonists. *Circulation Research* **55**, 336–348.

SNUTCH, T. P., LEONARD, J. P., GILBERT, M. M. & LESTER, H. A. (1990). Rat brain expresses a heterogeneous family of calcium channels. *Proceedings of National Academy of Sciences of the USA* **87**, 3391–3395.

SWANDULLA, D. & ARMSTRONG, C. M. (1988). Fast-deactivating calcium channels in chick sensory neurones. *Journal of Physiology* **92**, 197–218.

THAYER, S. A., WELCOME, M., CHHABRA, A. & FAIRHURST, A. S. (1985). Effects of dihydropyridine calcium channel blocking drugs on rat brain muscarinic and α-adrenergic receptors. *Biochemical Pharmacology* **34**, 181–188.

TSIEN, R. W., LIPSCOMBE, D., MADISON, K. R., BLEY, K. R. & FOX, A. P. (1988). Multiple types of neuronal calcium channels and their selective modulation. *Trends in Neurosciences* **11**, 431–438.

TSUNOO, A., YOSHII, M. & NARAHASHI, T. (1986). Block of calcium channels by enkephalin and somatostatin in neuroblastoma–glioma hybrid NG108–15 cells. *Proceedings of the National Academy of Sciences of the USA* **83**, 9832–9836.

WESTENBROEK, R. E., AHLIJANIAN, M. K. & CATTERALL, W. A. (1990). Clustering of L-type Ca channels at the base of major dendrites in hippocampal pyramidal neurons. *Nature* **347**, 281–284.